Master Thesis
by

Gerasim Khachatryan

Spectroscopic Derivation of the Stellar Surface Gravity

Supervisors:

Nuno C. Santos – *CAUP & DFA/FCUP*
Sérgio A. G. Sousa - *CAUP*

Centro de Astrofísica da Universidade do Porto, Rua das Estrelas, 4150-762, Porto, Portugal.
Faculdade de Ciências da Universidade do Porto, Rua do Campo Alegre, 4169-007, Porto, Portugal.

CAUP - 2012

Spectroscopic Derivation of the Stellar Surface Gravity

Abstract

The thesis addresses a technique for the fast estimation of the stellar surface gravity of solar-type stars. It is important for stars to be characterized as best as possible using stellar parameters, which are then used to compare the observations with stellar theory.

In this work we generated a grid of data using a spectral synthesis method. MOOG was used to compute synthetic spectra for Mg I b lines at λ5167.32 Å, λ5172.68 Å and λ5183.60 Å, the Na I D lines at λ5889.95 Å, λ5895.92 Å, and the Ca I lines at λ6122.21, λ6162.17, and λ6439.08 Å whose wings are extremely sensitive to surface gravity changes.

A code was created which uses normalized observed spectra of FGK stars for a given effective temperature, and metallicity.

We used 150 stars randomly peaked from HARPS GTO program for which we were able to determined the surface gravity for 89 stars. The results derived by our method seems to be reliable for dwarf stars. We have also compared our results with the ones derived by other authors found in literature.

Acknowledgments

First of all I would like to express my deep gratitude to my family for being always present for me. God bless you.

I also would like to thank my supervisors: N. C. Santos and S. G. Sousa for giving me this challenging opportunity.

I could not finish these acknowledgments without thanking my friends for their support, help and especially for their friendship.

I would like to acknowledge the support from the CAUP-11/2011-BI fellowship with a project reference – ERC-2009-StG-239953.

Table of Contents

List of Figures

List of Tables

List of Appendix

1. Introduction

1.1. History

Like protons and neutrons in Nuclear Physics, stars are the fundamental constituents of the Universe, but in a much large-scale. In fact, any attempt of understanding the structure and evolution of the Universe is constrained by our knowledge of the structure and evolution of stars. Stellar physics benefited a lot from solar physics. Conversely, the study of the Sun depends in many aspects, especially the evolutionary one, on the study of solar-like stars. The fastly growing exoplanet field is the most recent astronomy topic where the impact of stellar physics has important consequences. The characterization of exoplanets is very sensitive to the atmospheric parameters of the hosting stars.

For obvious reasons, only the external layers of the stars are directly accessible to the observations. High quality observations combined with robust theoretical models together with strong data analysis techniques are the perfect recipe for a successful stellar characterization.

Along history different observational techniques have been developed, and high-resolution spectroscopy is one of the most powerful. It allows the determination of different fundamental stellar parameters, such as the effective temperature, surface gravity, metallicity, etc. The different spectroscopic methods have been developed where the Sun is usually taken as a calibration reference and different spectral lines may be used depending on the main objective of the work (Fuhrmann et al. 1997; Bruntt et al. 2010).

When comparing results in literature, it is easy to notice that the most poorly determined stellar parameter is the surface gravity. Our aim in this thesis project is to address a technique for the fast estimation of stellar surface gravity of solar-type stars. It is very important to characterize the stars as best as possible using the stellar parameters since this is the best way to compare observations with stellar theory.

Spectral lines are very useful for the determination of spectroscopic stellar parameters. There are several work devoted to the determination of spectroscopic stellar parameters with spectral absorption lines. The English philosopher Roger Bacon (1214 – 1294) was the first person to recognize that sunlight passing through a glass of water could be split into colors. William Hyde Wollaston (1766 – 1828) was an English chemist and physicist. In 1802, in what was to later lead to some of the more important advances in solar physics, he discovered the spectrum of sunlight is crossed by a number of dark lines. This is considered to be “A Great Moment in the History of Solar

Physics" since it was the birth of Solar Spectroscopy.

1.2. Spectroscopy

The first evidence of existing terrestrial chemical element in an extraterrestrial body was the discovery of Sodium in the Sun. This was one of the major steps in Astrophysics. It was only possible by using the Spectroscopy technique. With this technique we can go beyond the simple detection of the elements, we can also quantify them. To do so we need also theoretical models of stellar atmospheres, that are used for the comparison with the observed spectra. In this way we can derive several important stellar parameters, such as the effective temperature, surface gravity and the elemental abundances (metallicity).

One of the most important parameters in stellar astrophysics is effective temperature. However, this parameter can be very difficult to measure with high accuracy, especially for stars that are not closely related to our very own Sun. Also correctly (or incorrectly) determining this parameter will have a major effect on the determination of other associated parameters, such as the surface gravity and the chemical composition of the associated star.

It is well-known that strong lines with pronounced wings can be good tracers of the stellar gravity (e.g. Gray 1992). Cayrel & Cayrel (1963) employed the pressure-dependent Mg Ib lines λ5172 and λ5183 in ϵ Virginis (G8III) as gravity indicator, and, more specific, Cayrel de Strobel (1969) presented the Mg Ib triplet lines as one of the best gravity criteria for late type stars.

Smith, Edvardsson & Frisk (1986) determined the surface gravity parameter from the pressure-broadened Ca I line λ6162 in their analysis of α CenA (G2 V) and α CenB (K0 V), followed by τ Ceti (G8 V) and η CasA (G0 V) in Smith &Drake (1987), the K0 giant Pollux (Drake&Smith 1991), the G8 subdwarf Groombridge 1830 (Smith et al. 1992) and the K2 dwarf ϵ Eridani (Drake & Smith 1993).

Most remarkable, however, is the work of Edvardsson (1988a, 1988b), who compared the strong line method to the ionization equilibrium method. His elaborate study made use of strong lines from Fe I and Ca I λ6162 applied to a sample of 8 nearby subgiants with α CenA+B and Arcturus included. As a result, the surface gravities derived from the ionization equilibrium of iron and silicon are found to be systematically lower than the strong line gravities. This, as Edvardsson proposes, may be an effect of errors in the model atmospheres, or departures from LTE in the ionization equilibria. Since then many abundance analysis of late stars have been done. But except for few investigations – such as those mentioned above – most of them do not take advantage of the wealth of information stored in

the wings of strong lines.

In Fuhrmann et al. (1997) work they propose to employ the pressure-broadened Mg I b lines to derive the gravity parameter for F and G stars on the base of high-resolution spectra and standard model atmosphere analysis. These lines were advocated to be a more robust and reliable tracer compared to the ionization equilibrium of Fe I/ Fe II, which is susceptible to over-ionization effects and uncertainties in the temperature structure of the model atmosphere.

By means of the strong Mg I b lines and in conjunction with others, rather weak, Mg I lines Fuhrmann et al. (1997) endorse in what follows that the strong line method is able to earmark the surface gravity in a very reliable way.

Also in Bruntt et al. (2010) work was described the method of determination of effective temperature and surface gravity with Fe_{I-II} lines. In this paper they describe the models, line list etc. used for calculations. Also they use broad lines for determination of surface gravity. The selected lines are extremely sensitive to the variation of the surface gravity. They have presented a detailed spectroscopic analysis of the planet-hosting star CoRoT-7. The analysis is based on HARPS spectra, that have higher S/N and better resolution than the UVES spectrum used to get a preliminary result (LRS09). They analysed both individual spectra from different nights and co-added spectra, and found excellent agreement. Only for one of the single HARPS spectra they found a systematic error in Teff and logg, which is explained by the low S/N. They described in detail the Versatile Wavelength Analysis (VWA) tool used to determine of the atmospheric parameters Teff and log g with Fe_{I-II} lines and the pressure sensitive Mg Ib and Ca lines. They used the SME tool to also analyse the Balmer and Na I lines. The method on which was based the determination of logg in this paper was spectral synthesis method.

Spectral lines were used also in Sousa et al. (2010) work to derive the effective temperature for solar type stars through an equivalent width ratios. The calibration was done for 433 line equivalent width ratios built from 171 spectral lines of different chemical elements. In this work presented a different approach with spectroscopy, where the temperature can be quickly estimated with high precision through line ratios. The equivalent width intrinsically has more information than line depths and can show significant differences in the calibrations. Nevertheless, his work is inspired by the following statement: “There is no doubt that spectral lines change their strength with temperature, and the use of the ratio of the central depths of two spectral lines near each other in wavelength has proved to be a near optimum thermometer” (Gray 2004). Therefore the ratio of the equivalent widths of two lines that have different sensitivities to temperature is an excellent diagnostics for measuring the temperature in stars or to check the small temperature variations of a given star. Although the effective

temperature scale can still be questioned, as with other methods, this method allows to reach a precision for the temperature down to a few Kelvin in the most favorable cases (e.g. Gray & Johanson 1991; Strassmeier & Schordan 2000; Gray & Brown 2001; Kovtyukh et al. 2003). Here the equivalent width (EW) was used to measure the line strength.

In this work we used spectral synthesis method to make a grid of spectral regions around strong and surface gravity sensitive lines.

The synthesis was done for eight spectral lines (Table 1) which are extremely sensitive to the surface gravity variation. Also, we will describe a code to find the stellar surface gravity using this grid.

Table 1. Spectral lines used in our work.

Line	Wavelength [Å]
Mg I b	5167.32
	5172.68
	5183.60
Na I D	5889.95
	5895.92
Ca I	6122.21
	6162.17
	6439.08

In section 2 we describe the tools and atomic parameters which were used in our calculations. The atomic parameters were extracted from VALD. The description of the VALD, interface, requests, and the structure and the format of VALD line data is given in subsection 2.1. In our calculations we took into account the Van der Waals broadening which is described in subsection 2.2. The description of the MOOG which we used to make a grid is in subsection 2.3. The sub-subsections describe the details which were used in MOOG.

The surface gravity determination is described in section 3. The subsections contain the description of the parameters which were used and determined in our work, adjusting the Van der Waals parameter for each line according to the χ^2 minimization, and the selection of “stable” part of the wing.

The description of the grid described in section 4 with subsections of determination of WD

(Wing Depth), which will be calculated from normalized spectra and will be used in determination of surface gravity as input parameter.

In section 5 we tested the first grid, which was made with two fixed parameters (metallicity and microturbulence velocity). The test was done for different values of microturbulence and rotational velocities. The impact of velocities on the shape of the line is described in subsection 5.1 and 5.2. The improving of the grid is described in section 6. In subsections we described the elemental abundances and the presence of metallicity in our grid. Finally the discussion and conclusion of the work is given in section 7.

2. Tools and Atomic parameters

2.1. VALD: The Vienna Atomic Line Data base

The "Vienna Atomic Line Data Base[1]" (VALD) consists of a set of critically evaluated lists of astrophysically important atomic transition parameters and supporting extraction software. VALD contains about 600.000 entries and is one of the largest collections of accurate and homogeneous data for atomic transitions presently available. It also includes specific tools for extracting data for spectrum synthesis and model atmosphere calculations. The different accuracies of data available in the literature made it necessary to introduce a ranking system and to provide a flexible method for extracting the best possible set of atomic line parameters for a given transition from all the available sources. The data base is presently restricted to spectral lines which are relevant for stars in which the LTE approximation is sufficient and molecular lines do not have to be taken into account. The provision was made that these requirements should not restrict the general design of VALD and the possibility of future expansion. In the paper of Piskunov et al. (1995) they describe the structure of VALD, the available data sets and specific retrieval tools. The electronic-mail interface (VALD-EMS) created to allow remote access to VALD is also described. Both users and producers of atomic data are invited to explore the database, and to collaborate in improving and extending its contents.

2.1.1. Structure and the format of VALD line data

The data base is built from several lists of atomic line data published by various providers. These *input lists* (or *source lists*) are preserved separately and are at first ranked according to their known performance in applications (predominantly in astrophysics), as well as according to error estimates provided by the authors of the original data. Comparisons were made by the VALD team to decide on the final ranking. Lists were also re-ranked according to their actual performance as part of the data base or wherever new data were included which supply information about the same atomic species.

Each individual request to the data base is handled by merging data from all relevant lists available. The merging procedure is performed by selecting each data for an individual spectral line

1 http://www.astro.uu.se/~vald/php/vald.php

from the most highly ranked list which provides information on the particular atomic parameter. This selection is preferred over averaging the data, because individual errors of line data from different sources can vary dramatically, like oscillator strengths (log gf-values) obtained from semi-empirical calculations (Figure 1) which would then be mixed up with high accuracy laboratory data. Moreover, for most of the line data individual error estimates are not available. Weighted averaging is recommended only when such estimates are known for all individual lines from two or more line lists which are supposed to be merged. On several occasions this has been done to create new VALD line lists which appear to the merging procedure of a VALD request as a single line list, although they were composed from several individual source lists. Sometimes, line data had to be corrected for systematic deviations (usually, but not always, known from the literature) before becoming part of the VALD archive. Thus, it was possible to enlarge, for instance, the number of lines for which reliable oscillator strengths with individual error estimates are available.

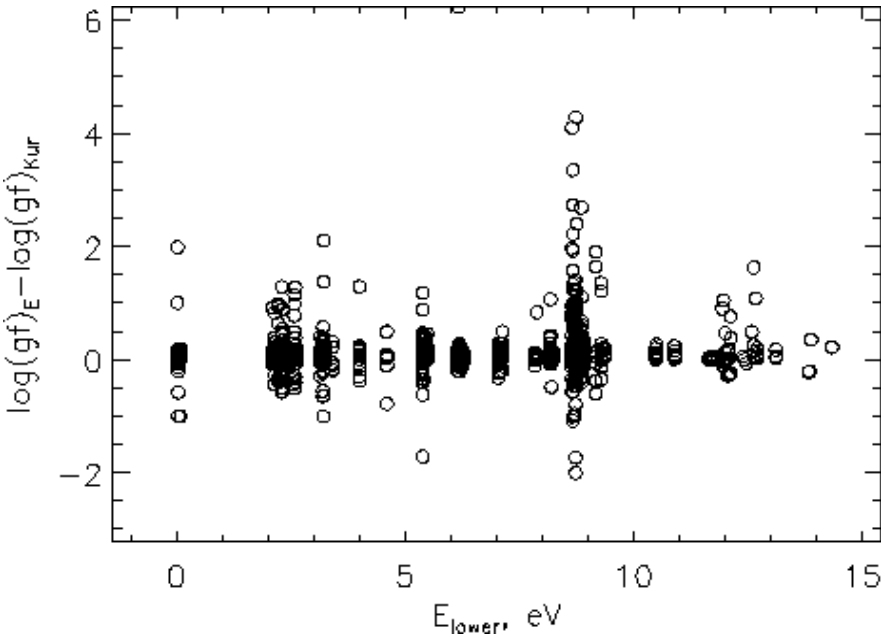

Figure 1. Dependence of the differences in log(gf) calculated by Ekberg and by Kurucz for CrIII lines on the excitation energy of the lower level (F. Kupka et al. 1999)

As a consequence, it became necessary to extend the information stored with each spectral line archived in VALD and a spectral line now is characterized by the following parameters (F. Kupka et. al. 1999):

1. Central wavelength in Å.
2. Species identifier. Provides element (or molecule) name and ionization stage.
3. Log gf - logarithm of the oscillator strength f times the statistical weight *g* of the lower energy level.
4. E_i - excitation energy of the lower level (in eV).
5. J_i - total angular momentum quantum number of the lower energy level.
6. E_k - excitation energy of the upper level (in eV).
7. J_k - total angular momentum quantum number of the upper energy level.
8. g_i - Lande factor of the lower energy level; default value is 99, if no value can be provided.
9. g_k - Lande factor of the upper energy level; default value is 99, if no value can be provided.
10. $\log \Gamma_r$ - logarithm of the radiation damping constant in s^{-1}; default value is 0, if no value can be provided.
11. $\log \Gamma_s$ - logarithm of the Stark damping constant in $(s\ N_e)^{-1}$ (i.e. per perturber) at 10000 K; default value is 0, if no value can be provided.
12. $\log \Gamma_w$ - logarithm of the Van der Waals damping constant in $(s\ N_H)^{-1}$ (i.e. per perturber) at 10000 K; default value is 0, if no value can be provided.
13. Spectroscopic terms of lower and upper energy levels.
14. Accuracy for log gf in dex (where available).
15. Comments.
16. Flags. Will be used to provide a link to information on Zeeman patterns, on autoionization lines, to information available for computing more accurate Stark and Van der Waals broadening parameters, to supplement the main quantum numbers for hydrogen lines, and more.

A VALD request consists of two parts: the type of request (Show line, Extract All, Extract element and Extract stellar) and the parameters of extraction (Figure 2).

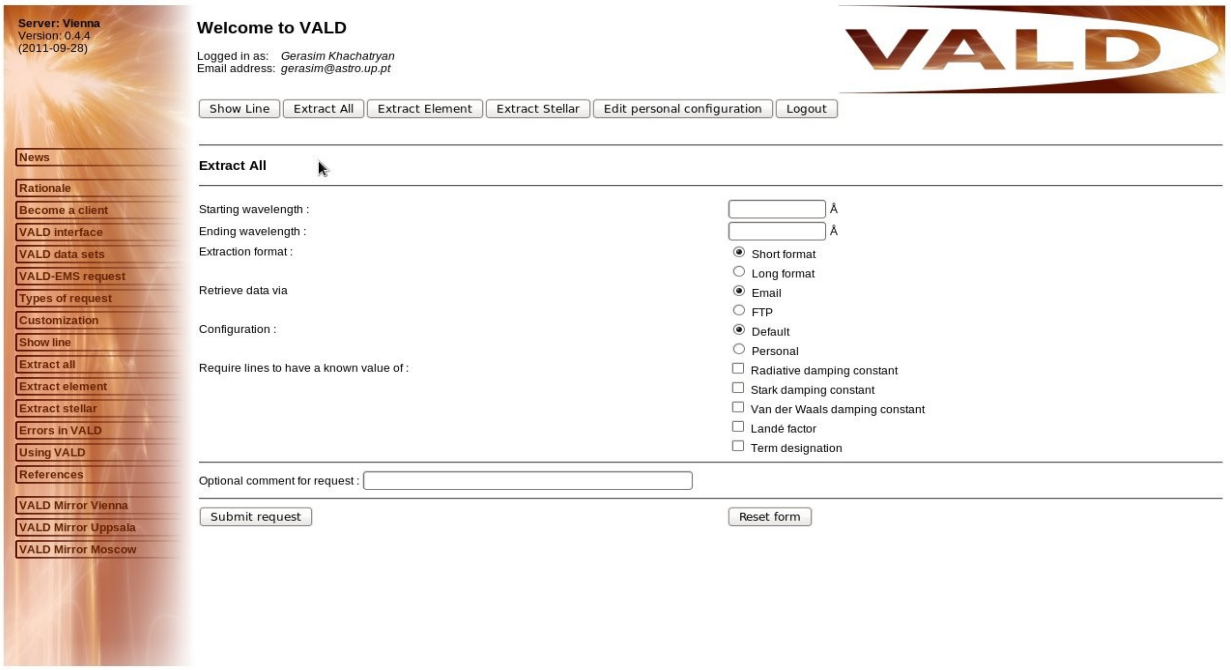

Figure 2. The Vienna Atomic Line Data Base (VALD) interface[1].

For example, the «Extract All» request will extract all atomic lines data in a given spectral range. The resulting extraction procedure will create a list similar to the list in Table 2.

Table 2. The line list extracted from VALD by «Extract All» request

Damping parameters Lande
Elm Ion WL(A) Excit(eV) log(gf) Rad. Stark Waals factor References
'P 1', 5166.0290, 6.9360, -2.000, 0.000, 0.000, 0.000,99.000,' 1 1 1 1 1 1 1'
'N 1', 5166.0360, 11.7580, -2.460, 0.000, 0.000, 0.000,99.000,' 2 2 2 2 2 2 2'
'Sm 2', 5166.0360, 1.3760, -0.800, 0.000, 0.000, 0.000, 1.540,' 3 4 4 4 3 4 3'
'Co 1', 5166.0600, 4.2590, -0.502, 8.033,-5.624,-7.705, 1.020,' 5 5 5 5 5 5 5'
'Tm 2', 5166.0820, 4.8540, -3.450, 0.000, 0.000, 0.000,99.000,' 6 6 6 6 6 6 6'
...
References:
1. Bell light: Si to K
2. Bell light: Li to O
3. Bell heavy: La to Lu & g_Lande
...

2.2. Pressure broadening: Van der Waals broadening

Van der Waals broadening is a pressure broadening due to the collisions of the atoms absorbing the light and other particles. The strengths and shapes of spectral lines contain a great deal of information about the stars, and the line absorption coefficient plays a fundamental role here. The situation in this regard is similar to the effect on the continuous absorption coefficient has on the shape of the continuum. Several different physical effects can enter the structuring of the final absorption coefficient.

The term pressure broadening implies a collisional interaction between the atoms absorbing the light and other particles. The other particles can be ions, electrons, or atoms of the same element as the absorbers or another type, or in cool stars, they might be molecules.

Depending on the distribution of encounter separations, and the shape of the energy curves, the net effect of all the absorbers along a line through the stellar photosphere can result in line shifts, asymmetries, and broadening.

The change in energy induced by the collision can often be approximated by a power law of the form (Gray 2008):

$$\Delta W = constant / R^n \qquad (1)$$

where the integer *n* depends on the type of interaction, and *R* is the distance to the perturber. Table 3 gives a summary of the types of interactions that are more important in stars.

Table 3. Types of pressure broadening.

n	Type	Lines Affected	Perturber
2	Linear Stark	Hydrogen	Protons, electrons
4	Quadratic Stark	Most lines, especially in hot stars	Ions, electrons
6	Van der Waals	Most lines, especially in cool stars	Neutral hydrogen

We can convert the energy change given in equation (1) to a change in frequency in the spectrum by subtracting the equation for the lower level from the equation for the upper level,

$$\Delta\nu = \frac{C_n}{R^n} \qquad (2)$$

The interaction constant C_n must be measured or calculated for each transition and type of interaction. It is known for only a few lines.

2.2.1. Numerical value for collisions with neutral perturbers

Neutral hydrogen is by far the dominant perturber for stars cooler that about 10 000 K. Also the classic Van der Waals formulation with n=6 in equation (2) has now been largely superceded. Typically, the Van der Waals formulation gives damping constants that are about a factor of 1.5 - 2 too small, but the error varies substantially from one line to the next, in the range from ~0.1 to ~5.

Using

$$\gamma_4 \approx 39 \mathrm{v}^{1/3} C_4^{2/3} N \qquad (3)$$

where γ is the dumping constant, v is the average relative velocity of atom of mass m_A and perturber of mass m_p, C is the interaction constant mentioned above, and N is the number of perturbers per unit volume.

Equation (3) is for quadratic Stark effect (n=4),

The impact parameter ρ_0 given by

$$\rho_0 = \left[\frac{2\pi \mathrm{C}_n}{v} \int_{-\pi/2}^{\pi/2} \cos^{n-2}\theta \, d\theta \right]^{1/(n-1)}$$

and for n=6 (see Table 3)

$$\int_{-\pi/2}^{\pi/2} \cos^{n-2}\theta \, d\theta = 3\pi/8$$

we are led to

$$\gamma_6 \approx 17 \mathrm{v}^{3/5} C_6^{2/5} N \qquad (4)$$

Using v_H to denote the velocity of hydrogen atoms,

$$\gamma_6 \approx 17 \mathrm{v}_H^{3/5} C_6^{2/5} 3 \left[\frac{1}{1 + \Phi_H(T)/P_e} \right] N_H$$

in which N_H represents the total number of hydrogen particles, neutrals and ions, and the factor *i* parentheses takes into account the ionization of hydrogen since only the neutrals cause the perturbations ($\Phi_H(T)/P_e = N_1/N_0$ is the ionization equation ($\Phi_H(T)$ is the ionization potential)). Using typical masses in equation

$$v = \left[\frac{8\mathrm{kT}}{\pi} \left(\frac{1}{m_A} + \frac{1}{m_p} \right) \right]^{1/2}$$

the expression reduce to

$$\log \gamma_6 \approx 20 + 0.4 \log C_6 + \log P_g - 0.7 \log T \qquad (5)$$

for P_g in dyne/cm^2. Unsöld (1955) showed how to evaluate the perturbation energy in an approximate way. The difference between the energies for the two levels of the transition leads the expression

$$C_6 = 0.3 \times 10^{-30} \left[\frac{1}{(I - \chi - \chi_\lambda)^2} - \frac{1}{(I - \chi)^2} \right] \qquad (6)$$

where *I* is the ionization potential and χ is the excitation potential of the lower level in electron volts for the atom of interest. The symbol $\chi_\lambda = h\nu = 1.2398 \times 10^4 / \lambda$ with λ in angstroms, and is the energy of a photon in the line" (Gray 2008).

One of the most used methods to derive spectroscopic parameters such as effective temperature, surface gravity and metallicity is based on the measurement of Fe I and Fe II week

absorption lines. These are then used to compute abundances using models that assume LTE for solar type stars and then the parameters are derived forcing excitation and ionization balance for the iron. This method works very well for FGK stars, specially for the effective temperature and metallicities.

2.3. MOOG – An LTE stellar line analysis program[2]

MOOG is a code that performs a variety of LTE line analysis and spectrum synthesis tasks. The typical use of MOOG is to assist in the determination of the chemical composition of a star. The basic equations (used in MOOG) of LTE stellar line analysis are followed, in particular using the formulation of Edmonds (1969).

The code is written in several subroutines that are called from a few driver routines: these routines are written in standard FORTRAN 77. One of the chief assets of MOOG is its ability to do on-line graphics. MOOG uses the graphics package Super Mongo, chosen for its easy implementation in FORTRAN codes. Plotting calls are concentrated in a few routines, and it should be possible for users of other graphics packages to substitute with other appropriate FORTRAN commands.

In our spectral analisis we basically make use of the *synth* driver for MOOG that is used for computing synthetic spectra. In order to use MOOG we need to include a stellar model. The ones used in our analysis are obtained from a grid of Kurucz Atlas 9 plane-parallel model atmospheres (Kurucz, 1993).

2.3.1. Drivers in MOOG

As described before MOOG is a FORTRAN code that performs a variety of LTE line analysis and spectrum synthesis tasks. The typical use of MOOG is to assist in the determination of the chemical composition of a star (Sneden 2002).

To run MOOG, we just need simply type «MOOGSILENT» or «MOOG» on our machine for interactive routine in the appropriate directory and the name of the driver (*Synth.par*). The program will then ask us questions about various input and output files. The first question always will ask for the name of the «parameter file» in which we have specified which driver to use. Depending on that driver

2 http://www.as.utexas.edu/~chris/moog.html

specification, MOOG will ask for other files. It is always necessary to input a «model atmosphere file», and almost always a «line data file». Other files will be called for as needed, including several output files that can be new names or the names of old files that are to be overwritten.

The driver is an important component of a MOOG run. This file tells MOOG which driver to use, how to process the data, and how to output the results.

The first line of the parameter file is the name of the driver program to be used. The current drivers are:

synth → spectrum synthesis, varying atomic abundances
isotop → spectrum synthesis, varying isotopic abundances
plotit → re-plotting of spectra that were created in a prior run
abfind → force fitting abundances to match single-line equivalent widths
blends → force-fitting abundances to match blended-line equivalent widths
cog →curve-of-growth creation for individual lines
cogsyn → curve-of-growth creation for blended features
ewfind → calculation of equivalent widths of individual lines
calmod → converting a BENG tauross model to an equivalent tau5000 scale
doflux → plot the overall flux curve of the model atmosphere
mydriver → dummy *drive,* user can substitute a specialty *driver* with this subroutine name

After the driver is named, the user may set values for any of the following parameters.

For the input files, if you specify a non-existent file name, then MOOG will ask you for the right name as it runs.

standard_out – 'string' – the filename for the standard (verbose) output file
summary_out – 'string' – the filename for thee EW summary OR the raw synthesis output
smoothed_out – 'string' – the filename for the smoothed synthetic spectrum output
model_in – 'string' – the filename for the input model atmosphere
lines_in – 'string' – the filename for the input line list
observed_in – 'string' – the filename for the input observed spectrum

2.3.2. *Synth* in MOOG

Synth is the other standard running option of MOOG which computes a set of trial synthetic spectra and (if the user so desires) matches these to an observed spectrum. Abundances can be deduced either by visual inspection of the plot or by mathematical minimization of the observed-computed spectrum difference.

Example of synthetic spectrum computations and their comparison to an observed spectrum is shown in Figure 3.

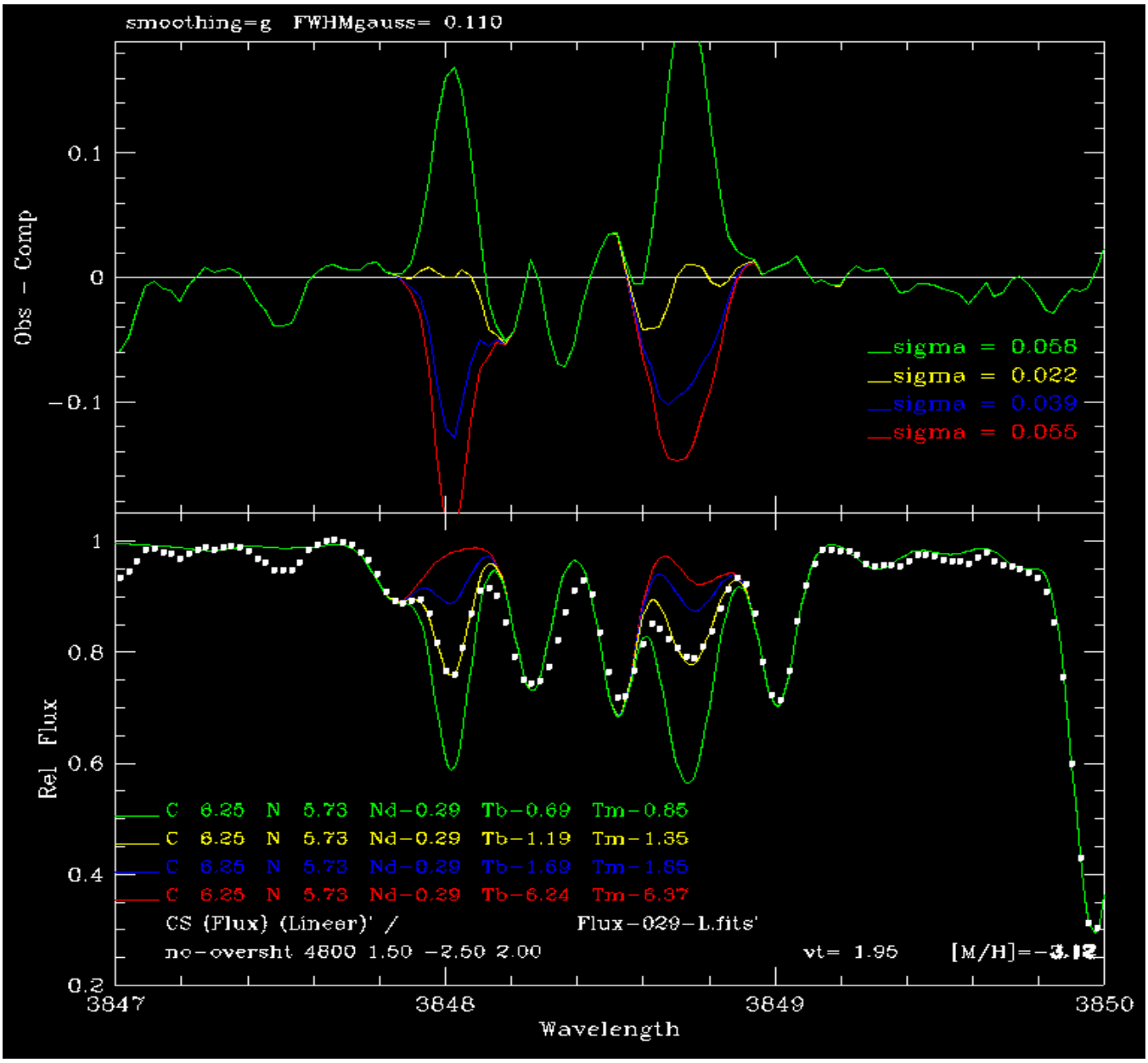

Figure 3. This spectrum contains a complex blend of weak CN molecular lines and significant features of rare earth species, Ce II, Nd II, Sm II, Tb II, and Tm II. Some abundances have been altered from their input values, as listed in the figure legend, and the abundances of Tb and Tm have been varied for each synthesis. the colored lines represent the four synthetic spectrum computations, and the white dots represent the observed spectrum. The bottom panel shows the spectra plotted together, and the top panel shows the "o-c" comparisons of synthetic and observed spectra. The abundance units are logarithmic number densities on a standard scale in which logε(H)=12.

2.3.3. The inputs of SYNTH driver

In section 2.3.2 we bring a brief description of *synth* driver which is used to compute a set of trial synthetic spectra.

We have used *synth* driver for computing synthetic spectra. The program written for *synth* driver is shown in Table 4. MOOG will produce a synthesis of a 6 Å stretch of spectrum, including the [Ca I] feature at 6439.08Å.

Table 4. Synth.par for computing synthetic spectra.

```
synth
standard_out      'standard_out'
summary_out       'summary_out'
smoothed_out      'smoothed_out'
model_in          'sun.atm'
lines_in          'VALD_6439.08'
observed_in       'sun_6439.08.ascii'
terminal          X11
atmosphere        1
molecules         2
lines             1
flux/int          1
plot              2
abundances        1     1
    26          0.0
synlimits
    6436.00     6442.00     0.01      5.00
obspectrum        5
plotpars          1
    6436.00     6442.00     -0.2      1.05
    0.0     0.000     0.000     0.0
    g     0.100     0.00      0.00      0.00      0.00
```

The first line is the name of the *driver* program to be used (*synth*), second, third and fourth lines are outputs of the program, model_in, lines_in, and observed_in are the input model, input line-list, and input observed spectra in .ascii format, respectively.

terminal: "terminal type": X11 – Sun OpenWindows, or any X11 (*sm*)

atmosphere: controls the way the model atmosphere is shown on the standard output file:

1 output standard information about the atmosphere

molecules: controls molecular equilibrium calculations:

2 do molecular equilibrium and output results

lines: controls the output of the line data:

1 output standard information about the input line list

flux/int:

1 perform central intensity calculations

plot: type of plot output:

2 plot synthetic and observed spectra (synthesis *driver* only)

abundances: abundances to override those set during the model atmosphere input. There are two required numbers on the line with this keyword; their meanings are:

i number of elements that diverge from the preset abundances

j number of different synthesis to be run (maximum=5)

synlimits: the wavelength parameters for synthesis. Only the keyword appears on this line. Then one the next line, four parameters must appear in the following order:

a the beginning synthesis wavelength/frequency

b the ending synthesis wavelength/frequency

c the wavelength/frequency step size in the synthesis

d the wavelength/frequency $\pm\Delta$ from a spectrum point to consider opacity contributions from neighboring transitions

obspectrum: indicates the type of the input observed spectrum:

5 an ASCII file, with lambda as x-coord, flux as y-coord

plotpars: allows the user to set all of the plotting parameters if they are reasonably well known in advance.

1 set the default plotting parameters in the next three lines

On the first line, four parameters are required:

a left edge (wavelength/frequency units) of the plot box

b right edge (wavelength/frequency units) of the plot box

c lower edge (relative flux units) of the plot box

d upper edge (relative flux units) of the plot box

On the second line, four parameters are required:

e a velocity shift to be applied to the observed spectrum

f a wavelength shift to be applied to the observed spectrum

g a velocity additive shift to be applied to the observed spectrum

h a velocity multiplicative shift to be applied to the observed spectrum

On the third line, six parameters are required:

i a one-character smoothing type for the synthetic spectra

j the full-width-at-half-maximum (FWHM) of a Gaussian smoothing function

k *vsini* for a rotational broadening function

l limb darkening coefficient of a rotational broadening function

m the FWHM of a macroturbulent broadening function

n the FWHM of a Lorentzian smoothing function

Permissible smoothing types are g (Gaussian), l (Lorentzian), v (rotational), m (macroturbulent), several combinations of these, and p (variable Gaussian).

We just entered *zeros* for *k, l, m,* and *n*. These are the parameters that are not needed to be chosen.

2.3.4. The Line Data File

In this line data file one designates all of the spectral features to take part in MOOG computations. The quantities desired are very straightforward, with only a few variations that depend on the particular MOOG driver to be employed. The file always begins with a comment line (see Table 5, VALD 6436-6442) which has no computational function. But like the atmosphere comment line, this line will be displayed in various plots and output files, so it pays to make it fairly informative. Then on succeeding lines of this files, spectral feature data are entered in either a formatted (7e10) or an unformatted manner, depending on the value of *freeform* in the parameter file. MOOG can hold the data for up to 500 spectral lines in memory at any one time. For doing synthetic spectra, there should be $\leq$500 lines included in the line opacity calculations at any one wavelength step.

Here are the line list input; the order of their appearance cannot be changed.

- Wavelength, always in Å.
- atomic or molecular identification (0 = neutral, 1 = singly ionized, etc.).
- line excitation potential, always in electron volts (eV).
- gf, or log(gf); MOOG figures out which form it is dealing with by looking for a negative

value for any one of the entries for gf.

- the Van der Waals damping parameter C6, or a factor to multiply an internally generated C6 value; this quantity is optional, and may be left blank in formatted reads.

In Table 5 shown as an example of a formatted line data file. Here is a part of a line list that would be used to generate synthetic spectra of a [Ca I] line:

Table 5. Example for the formatted line data file. First column is a wavelength, always in Å. Second column is an atomic or molecular identification. Third column is the line excitation potential, always in electron volts (ev). Fourth column is the value of log(gf), fifth column is a Van der Waals dumping parameter.

VALD 6436-6442				
6436.1110	25.2	26.8470	-1.968	-7.578
6436.1940	28.1	14.7300	-3.348	-7.584
6436.2060	28.1	14.7300	-2.758	-7.584
6436.3320	26.1	12.8880	-6.726	-7.300
6436.3380	26.1	12.8880	-8.555	-7.300
6436.3940	26.0	5.5380	-8.801	-7.180
....				
6439.0750	20.0	2.5260	0.390	-7.700
....				
6441.9050	23.0	3.3150	-1.907	-7.617
6441.9100	24.0	4.2070	-2.538	-7.830
6441.9710	28.1	14.8990	-3.079	-7.589
6441.9750	23.2	19.3840	-0.959	-7.796

2.3.5. Local Thermodynamic Equilibrium – LTE

In thermodynamics, a system is in equilibrium when it is in:

- thermal equilibrium,
- mechanical equilibrium,
- radiative equilibrium, and
- chemical equilibrium.

Equilibrium means a state of balance. In a state of thermodynamic equilibrium, there are no net flows of matter or of energy, no phase changes, and no unbalanced potentials (or driving forces), within the system. A system that is in thermodynamic equilibrium experiences no changes when it is isolated from its surroundings.

In thermodynamics, exchanges within a system and between the system and the outside are controlled by intensive parameters. As an example, temperature controls heat exchanges. Local thermodynamic equilibrium (LTE) means that those intensive parameters are varying in space and time, but are varying so slowly that, for any point, one can assume thermodynamic equilibrium in some neighborhood about that point.

It is important to note that this local equilibrium may apply only to a certain subset of particles in the system. For example, LTE is usually applied only to massive particles. In a radiating gas, the photons being emitted and absorbed by the gas need not be in thermodynamic equilibrium with each other or with the massive particles of the gas in order for LTE to exist. In some cases, it is not considered necessary for free electrons to be in equilibrium with the much more massive atoms or molecules for LTE to exist.

In the Boltzmann equation can be used to represent the ratio between the number of atoms in a *n* level (N_n) and the total number of the same element (N):

$$\frac{N_n}{N}=\frac{g_n}{u(T)}10^{\theta(T)\chi_n} \qquad (7)$$

here, g_n is the degeneracy of level *n*, χ_n is the excitation energy of the same level, $\theta(T) = 5040/T$ and $u(T)=\sum g_i e^{\chi_i/kT}$ is the partition function, *k* is a Boltzmann's constant, and *T* is the temperature.

In the same way, Saha's Equation can be used to deal with the ionization of the elements for collision dominated gas:

$$\frac{N_{I+1}}{N_I}=\frac{1}{P_e}\frac{(\pi m_e)^{3/2}(2\mathrm{kT})^{5/2}}{h^3}\frac{u_{I+1}}{u_I}e^{-E_I/kT} \qquad (8)$$

where, N_{I+1}/N_I is the ratio between the number of ions in a given ionization, u_{I+1}/u_I is the ratio of respectives partition functions, m_e is the electron mass, h is the Plank's constant, P_e is the electron pressure, and E_I is the ionization potential.

Thermodynamic equilibrium is achieved when the temperature, pressure and chemical potential of a system are constant. LTE is assumed when these parameters are varying slowly enough in space and time. In these conditions each point emits like a black body with a given temperature *T*. This approximation is acceptable for the atmospheres of solar-type stars, since there are more transitions due to the collisions than radiation induced. On the external layers of the atmosphere it not valid because of big losses of energy on a star surface where photons can run without any hindrances.

2.3.6. Description of the model atmosphere

There are four different types of model atmosphere input that currently may be handled by MOOG. In any model atmosphere file, the first three lines of information are always the same:

line 1: a left-justified keyword that clues in MOOG to which atmosphere type is about to follow. Permissible model type keyword are 1) KURUCZ, for models generated with the ATLAS code (Kurucz 1993); 2) BEGN, for models generated with the MARCS code; 3) KURTYPE, for ATLAS-generated models that come without continues opacities even though they are on a «*rhox*» depth scale (this is a specialized model type); 4) KUR-PADOVA, for models with quantities arranged in a way for input from the Padova Observatory ATLAS program; 5) NEWMARCS, for newest MARCS models; and 6) GENERIC, for models that have a «*tau*» depth scale but no corresponding continuous opacities.

line 2. a comment line; it has no computational purpose, but will appear on various plots and outputs. So we should take a time to make this line informative.

line 3. the number of depth points. This is an integer ≤76 that can be put in any spaces after the first 10 spaces of this line.

The next set of lines (whose count depends on the number of atmosphere layers («ntau»)) are devoted to the model atmosphere physical quantities. These are slightly different in each model type case.

If model type is KURUCZ, which is our case, each of the next ntau lines contains these quantities in the following order: ρx (rhox), T, P_g, N_e, k_{Ross}. Here, all quantities have their usual meanings: ρx≡rhox is mass depth, T is the temperature, P_g is the gas pressure, electron number (N_e) and k_{Ross} is a Rosseland mean opacity on a mass scale. The proper way to get these data is simply to take the direct summary output from ATLAS run. MOOG is supposed to be clever enough to distinguish between the P_g and its logarithm, and between N_e, P_e or either of their logarithms, without any user invitation.

Mostly KURUCZ model is self-explanatory. The last number (0.00E+00) on each model atmosphere layer line is never read by MOOG. The other numbers on these lines are, in order, ρx , T, P_g, N_e, k_{Ross} , and the radiative acceleration (not used by MOOG). Example of KURUCZ model is shown in Table 6. Note the more extensive molecular equilibrium network that has been requested.

Table 6. Example of KURUCZ model atmosphere.

```
KURUCZ
        Teff= 5700        log g= 4.45
NTAU       72
 0.50531520E-03   3649.0 0.142E+02 0.274E+10 0.263E-03 0.756E-01 0.200E+06
 0.66145317E-03   3671.7 0.186E+02 0.353E+10 0.305E-03 0.793E-01 0.200E+06
 0.84169325E-03   3693.4 0.237E+02 0.441E+10 0.352E-03 0.816E-01 0.200E+06
 0.10505836E-02   3716.2 0.296E+02 0.544E+10 0.404E-03 0.828E-01 0.200E+06
 0.12934279E-02   3739.8 0.365E+02 0.662E+10 0.463E-03 0.824E-01 0.200E+06
          .                .                .                .             .
          .                .                .                .             .
0.76461163E+01   9557.7 0.216E+06 0.470E+16 0.534E+02 0.502E+01 0.200E+06
  0.79648285E+01        9740.1   0.224E+06   0.559E+16   0.643E+02   0.483E+01
0.200E+06
  0.83220358E+01        9904.0   0.234E+06   0.653E+16   0.757E+02   0.475E+01
0.200E+06
   1.000e+05
NATOMS     1   0.00
     26.0   7.47
NMOL      19
     606.0    106.0    607.0    608.0    107.0    108.0    112.0    707.0
     708.0    808.0     12.1  60808.0  10108.0    101.0      6.1      7.1
       8.1    822.0     22.1
```

We used programs, *intermod* and *transform*, to obtain a specific KURUCZ model atmosphere. The *intermod* program interpolate a grid of Kurucz Atlas plane-parallel model atmosphere (Kurucz 1993) and the *transform* program transforms the interpolated model into a MOOG format model ready to be used.

3. Surface gravity determination

As described before the surface gravity of late-type stars can be determined from the spectral lines given in Table 1, which are extremely sensitive to the surface gravity.

3.1. The Atomic Line Data

The atomic parameters was extracted from the Vienna Atomic Line Data Base (VALD). The data base is built from several lists of atomic line data. These source lists are preserved separately and are at first ranked according to their known performance in applications (predominantly in astrophysics), as well as according to error estimates provided by the authors of the original data.

We extracted atomic line data from VALD using “extract all” request giving the wavelength range. The corrections was done for the atomic line data (Table 2): chemical elements (first column in table) were changed with corresponding atomic number and ionization stage. We need to have a certain format and sequence of line data file for using in MOOG as an input.

In our calculations we used only few parameters mentioned before in section 2.1.1., e.g. central wavelength in Å, provides element (or molecule) name and ionization stage, excitation potential in EV, logarithm of the oscillator strength *f* times the statistical weight *g* of the lower energy level, and logarithm of the Van der Waals damping constant in $(s\ N_H)^{-1}$ (i.e. per perturber) at 10000 K; default value is 0, if no value can be provided.

3.2. Adjusting the Van der Waals constant

A spectral line extends over a range of frequencies, not a single frequency (i.e., it has a nonzero line-width). In addition, its center may be shifted from its nominal central wavelength. There are several reasons for this broadening and shift. These reasons may be divided into two broad categories - broadening due to local conditions and broadening due to extended conditions. Broadening due to local conditions is due to effects which hold in a small region around the emitting element, usually small enough to assure local thermodynamic equilibrium. Broadening due to extended conditions may result from changes to the spectral distribution of the radiation as it traverses

its path to the observer. It also may result from the combining of radiation from a number of regions which are far from each other.

Van der Waals broadening is a case of the broadening due to local effects. This occurs when the emitting particle is being perturbed by Van der Waals forces. For the quasi-static case, a Van der Waals profile is often useful in describing the profile.

In physical chemistry, the Van der Waals force (or Van der Waals interaction), named after Dutch scientist Johannes Diderik Van der Waals, is the sum of the attractive or repulsive forces between molecules (or between parts of the same molecule) other than those due to covalent bonds, the hydrogen bonds, or the electrostatic interaction of ions with one another or with neutral molecules.

Van der Waals constant has a strong influence on the shape of the spectral line. Bigger value of Van der Waals parameter can produce wider spectral line (Figure 4).

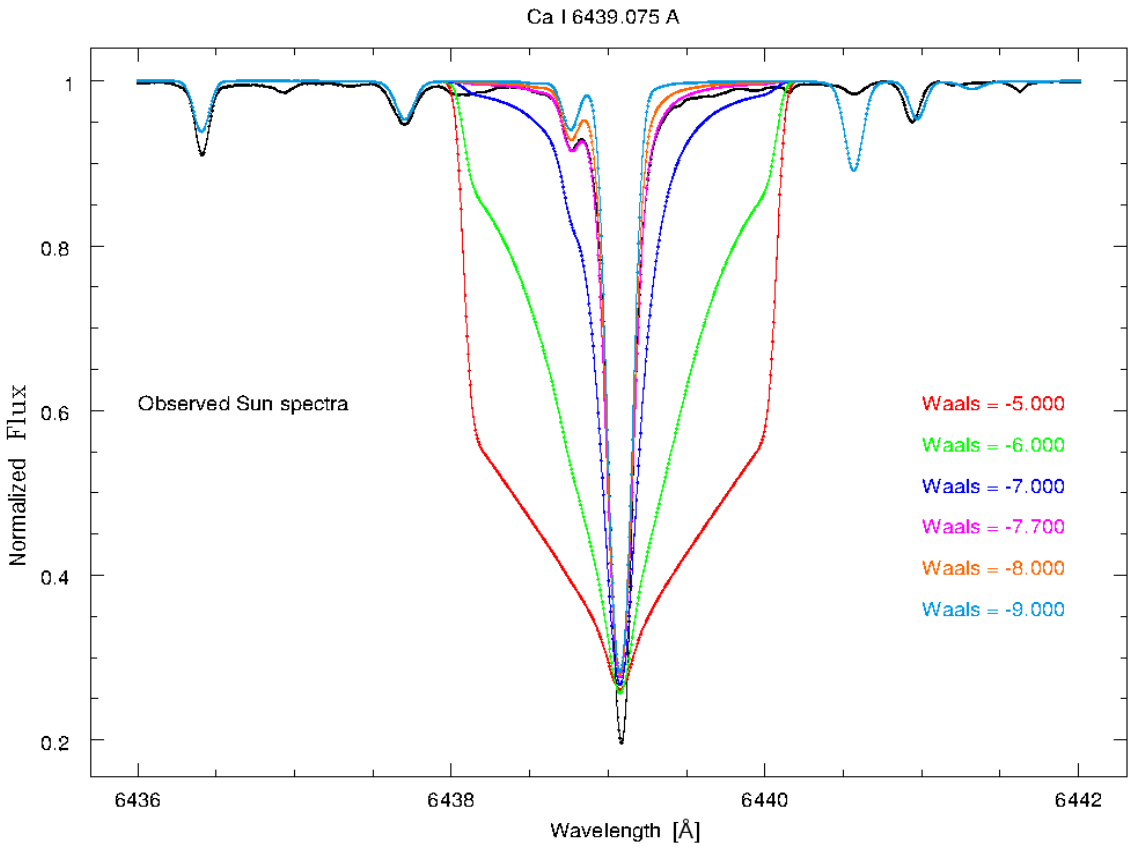

Figure 4. Observed Sun spectra (black line) in a given wavelength range fitted with synthetic spectra (colored lines) for different value of Van der Waals parameter for Ca I line at 6439.08 Å.

We followed the approach of Fuhrmann et al. (1997) to adjust the Van der Waals constants (pressure broadening due to the hydrogen collisions) by requiring that our reference spectrum of the Sun produce the solar value log g = 4.44.

The code was created to adjust the Van der Waals constant for each sensitive line according to the χ^2 minimization with an equation:

$$\chi=\sqrt{(\frac{1}{n})\sum_{i=0}^{N}(x-x_i)^2} \qquad (9)$$

at a special wavelength range. The atomic line data extracted from VALD were used as an input for MOOG to compute synthetic spectra with different Van der Waals parameter which was changed inside the program with cycle from -5.000 to -10.000 for each sensitive line.

The line list contains the Van der Waals constant as default for each line.

To determine the Van der Waals parameter we computed synthetic spectra for different values of the Van der Waals parameter. The values of the Van der Waals parameter was changed by steps of 0.02. Each new line list was saved and was used as an input for computation of synthetic spectra. The best value of Van der Waals parameter correspond to the best fit of synthetic spectra to the observed spectra. For realization of the minimization at first we need to choose the “stable” part of the wing (wavelength range), where we can apply our minimization approach according to the equation (9).

3.3. Selection of the “stable” part of the wing

The synthetic spectrum were computed for different values of effective temperature and surface gravity (5000K, 5700K, 6200K, 6500K for effective temperature and 2.0, 3.0, 4.44, 5.0 for surface gravity) Figure 5. The wavelength ranges, which was selected for χ^2 minimization according to the equation (9), were chosen by looking at the synthetic spectra by eye. We selected the most «stable» part of the synthetic spectra: the part of spectra which is not changing with temperature and surface gravity changes.

In Figure 5, if can be seen the small part of the spectra, at 6438.60Å – 6438.86Å, close to the central line 6439.08Å, is changing with different parameters. In each case a higher log g means the synthetic line become wider. In the Figure 5 the 6438.78Å line disappear for higher log g and lower

temperature (top left), but the same line with same *logg* exist in the plot for higher temperature (bottom left). So, the wavelength ranges which we selected at 6438.46– 6438.99Å and at 6439.17 – 6439.59Å are more stable. The same action was done for other wavelength from our selection.

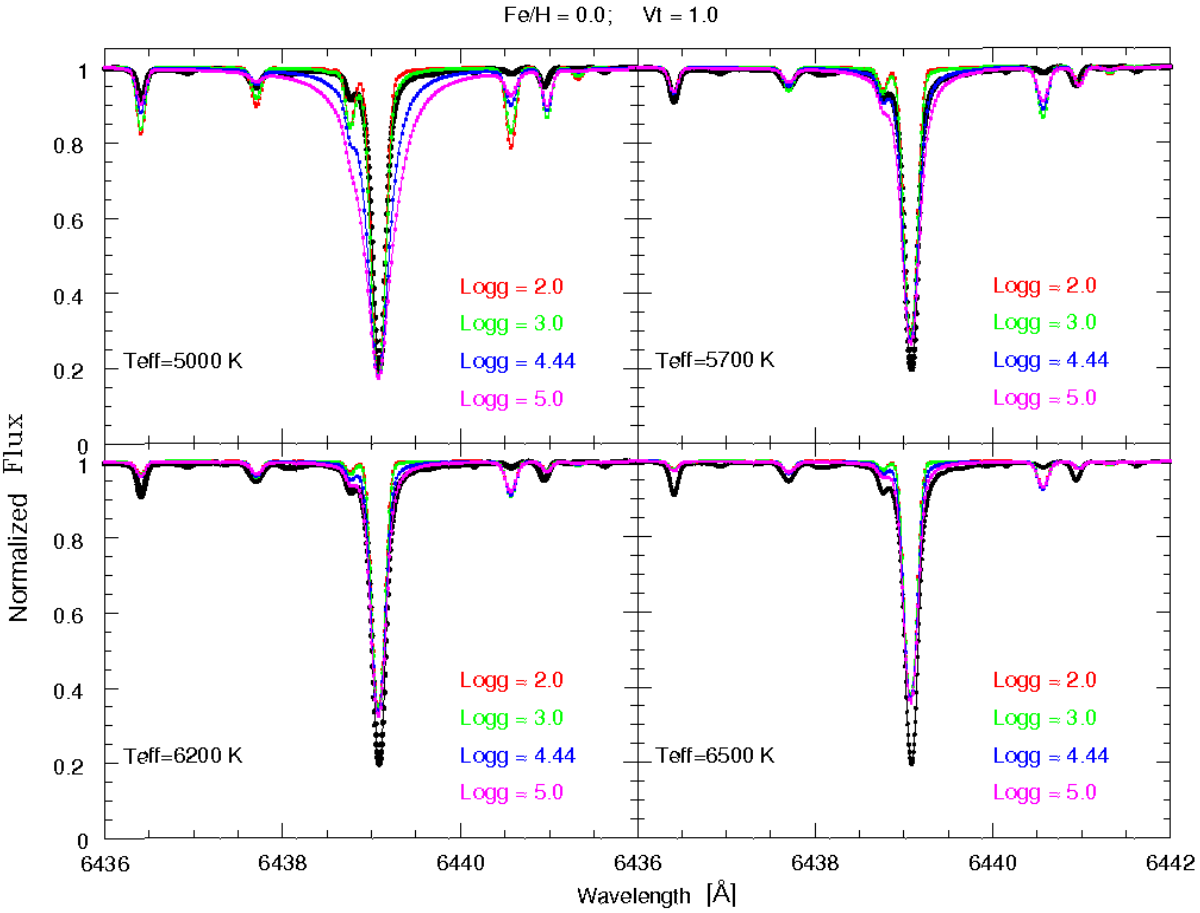

Figure 5. Sun spectra (black dotted line) with synthetic spectra (colored lines) for different temperature. Central line is a Ca I line at 6439.08Å.

The selected wavelength regions for the analysis of each line for determination of Van der Waals parameter is presented in Table 7.

Table 7. Atomic Lines with corresponding wavelength range for χ^2 minimization

Line	λ [Å]	Wavelength range
Mg I b	5167.32	5166.46 – 5167.03 5167.72 – 5168.03
	5172.68	5171.84 – 5172.22 5172.92 – 5173.41
	5183.60	5182.81 – 5183.37 5183.77 – 5184.12
Na I D	5889.95	5889.12– 5889.59 5890.14 – 5890.51
	5895.92	5895.32 – 5895.75 5896.10 – 5896.30
Ca I	6122.21	6121.52– 6122.10 6122.33– 6122.46
	6162.17	6161.54 – 6162.04 6162.30– 6162.94
	6439.08	6438.46– 6438.99 6439.17– 6439.59

For χ^2 minimization in a given wavelength range we need to have all point in both observed (Sun spectra) and computed synthetic spectra. For this we need to interpolate computed synthetic spectra to the observed Sun spectra. Synthetic spectra obtained by MOOG has a 0.02 step in a wavelength and observed Sun spectra has a 0.0065 step in a wavelength. We need to interpolate to recover all missed point in the synthetic spectra compared with observed Sun spectra. In particularly, for 6439.08 Å computed synthetic spectra line-list has 601 lines and observed Sun spectra line-list has 914 lines in a given wavelength range (6436.00 – 6442.00 Å).

We have used the quadratic Spline Interpolation which differs from approximation in the sense that the interpolated function *f* is forced to take the given values y_i in the given points x_i. For instance: a polynomial of degree n-1 can be fitted to go through data points (if $X_i \neq X_j$ $\forall i \neq j$). Splines are piecewise functions (often polynomials) with pieces that are smoothly connected together.

The output line list for each line with different Van der Waals parameter was interpolated to the Sun spectra. Comparison between Sun spectra and interpolated synthetic spectra was done automatically, according to the χ^2 minimization in a given wavelength range with equation (9). Selected wavelength range for χ^2 minimization is given in table 5. In the Figure 4 can be seen that

Waals=-7.700 (magenta dotted line) is a best fitted value for minimization. The black dotted line corresponds to the observed Sun spectra and colored lines correspond to the interpolated synthetic spectra.

In Table 8 we listed the adjusted Van der Waals parameters along with the values extracted from VALD. Following the convention of VALD, it is expressed as the logarithm (base 10) of the full-width half-maximum per perturber number density at 10000K.

The Van der Waals parameter was adjusted in Bruntt et al. (2010) work followed the approach of Fuhrmann et al. (1997) (Table 8).

Table 8. Adjusted Van der Waals constant compared to the values extracted from VALD and Bruntt's results

		log γ [rad cm^3/s]		
Line	**λ [Å]**	**Adjusted**	**VALD**	**Bruntt's results**
Mg I b	5167.32	-7.100	-7.267	-7.42
	5172.68	-7.300	-7.267	-7.42
	5183.60	-7.360	-7.267	-7.42
Na I D	5889.95	-7.620	-7.526	-7.85
	5895.92	-7.600	-7.526	-7.85
Ca I	6122.21	-7.240	-7.189	-7.27
	6162.17	-7.200	-7.189	-7.27
	6439.08	-7.700	-7.704	-7.84

The line lists were corrected according to the adjusted Van der Waals parameter and were used for further calculations.

4. Description of the Grid

4.1. Determination of the Wing Depth (WD)

Our goal is to determine spectroscopic surface gravity (logg) using specific lines of Na, Ca and Mg which are extremely sensitive to the surface gravity. For determination of surface gravity with spectral lines we calculate WD with equation (10). WD is the difference of the value of the flux of average point of the «stable» part of the wing from one (Figure 6).

$$WD = 1 - Flux(average\ point) \qquad (10)$$

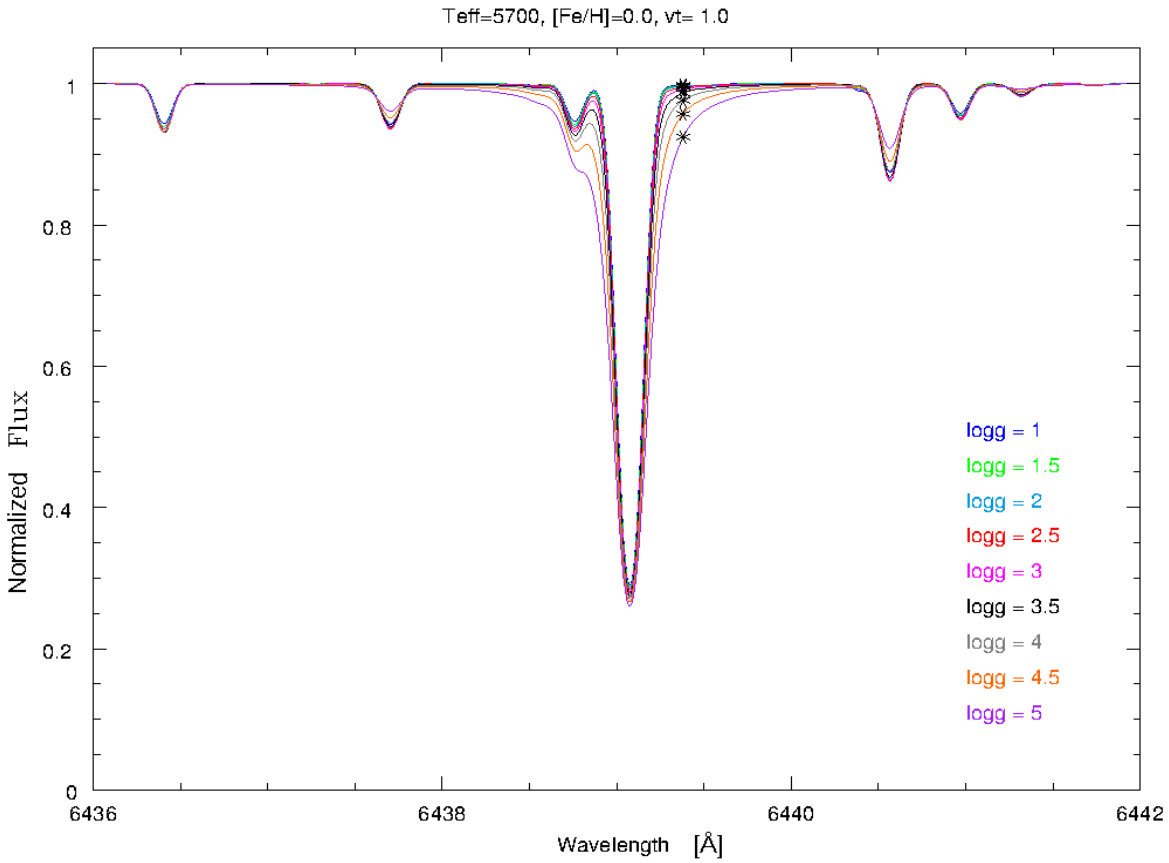

Figure 6. Synthetic spectra computed for different values of logg. Black asterisks present the average point of the “stable” part of the wing of each spectra.

As can be seen in Figure 6 for the same star with parameters mentioned at the top of the figure the line is wider for logg=5 dex than for logg=1 dex. The movement of the average point which marked on the figure as asterisks is smoothly and clear. The dependence of the quantity WD calculated by equation (10) is shown in Figure 7.

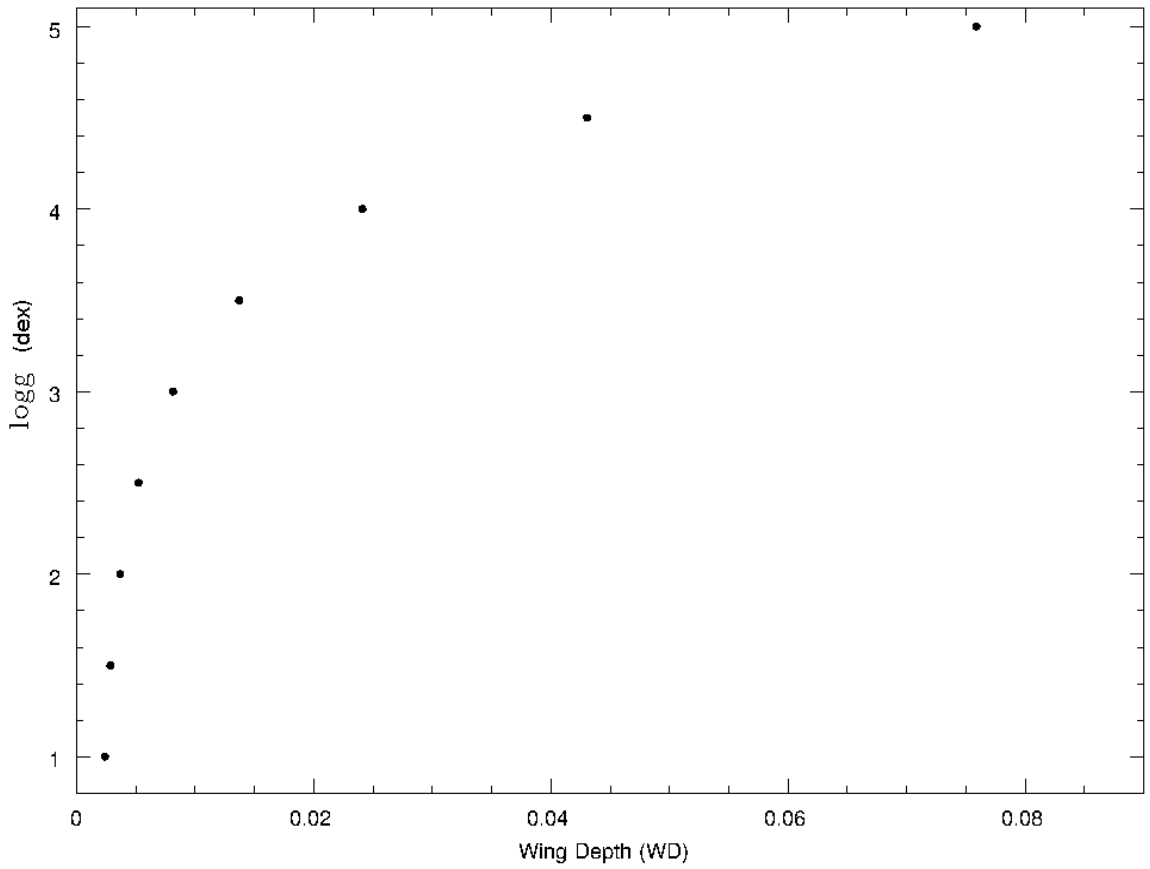

Figure 7. Dependence of the WD on surface gravity variety for a given temperature.

The wavelength of average point of each line is given in Table 9.

Table 9. Central lines with corresponding «stable» part of wavelength range and wavelength of an average point.

Line	«Stable» part of the wing	Average point
5167.32 Å	5167.72 – 5168.03	5167.88 Å
5172.68 Å	5172.92 – 5173.41	5173.17 Å
5183.60 Å	5183.77 – 5184.12	5183.95 Å
5889.95 Å	5890.14 – 5890.51	5890.32 Å
5895.92 Å	5896.10 – 5896.30	5896.20 Å
6122.21 Å	6122.33– 6122.46	6122.40 Å
6162.17 Å	6162.30 – 6162.94	6162.62 Å
6439.08 Å	6439.17 – 6439.59	6439.38 Å

4.2. “WD” 3D profile

The 3D distribution of WD for different Logg and different effective temperature shown in Figure 8 for central line 6439.08 Å. Metallicity and microturbulence velocity are fixed to 0.0 dex and 1.0 km/s respectively.

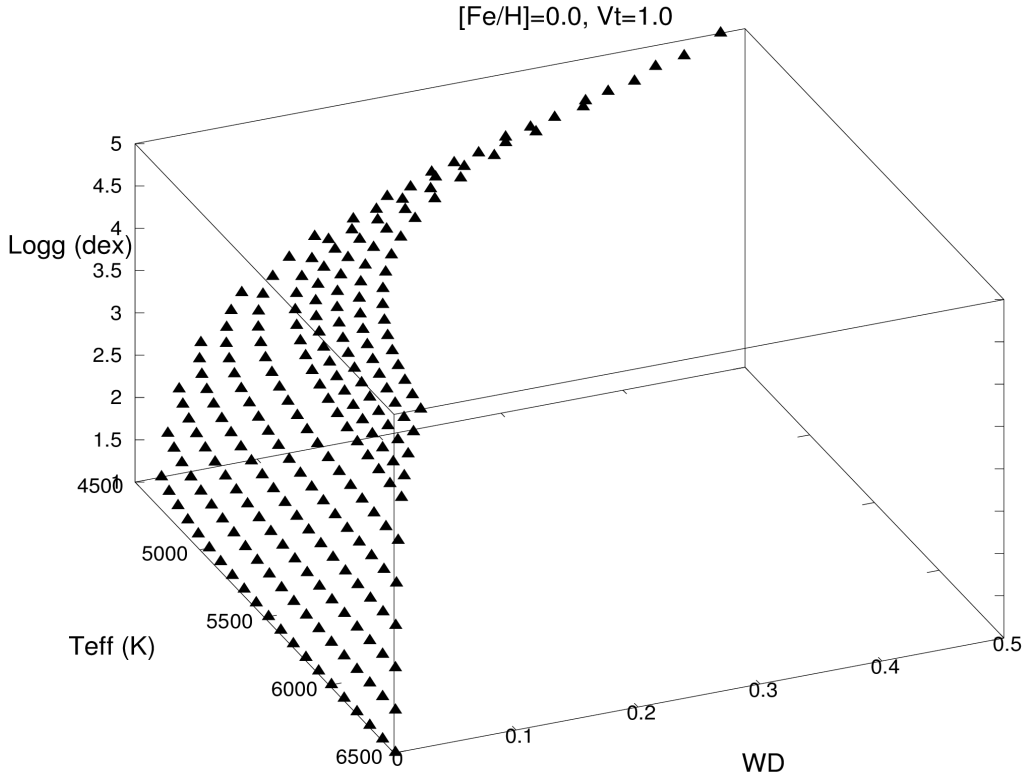

Figure 8. Distribution of WD for different logg and Teff for CaI line at 6439.08 Å.

As can be seen in the Figure 8 our grid has certain values of effective temperature and surface gravity, i. e. we have a model for effective temperature with step 100 from 4500 to 6500, which are containing logg from 1.0 to 5.0 and corresponding calculated value of WD. We selected the range of the effective temperature for solar-like stars and the step we choose too fill grid is 100 K which allowed us to have densely grid and with interpolation for any value of effective temperature reach to every model. The range for surface gravity include almost all possible values of stellar surface gravity which can have the stars.

The test was done for 5 stars to obtain preliminary result. The stars were chosen from HARPS GTO sample, for about 1.0 microturbulence velocity and close to solar metallicity (Table 10). The spectra of these stars were normalized to one in a given region for determination of WD.

Because the grid has specific steps, for any effective temperature between 4500 to 6500, we used interpolation with taking previous and next «models». For example for HD 28185 star which has an effective temperature 5667 K to find surface gravity, we have taken «model» with T_{eff}=5600 K and T_{eff}=5700 K and made an interpolation. The preliminary results are given in the Table 10. First column is the name of the stars, second column is the effective temperature of the stars, third column is the surface gravity of the stars determined by Sousa et al. (2008). Fourth column is the metallicity of the stars and fifth column is the surface gravity of stars calculated by our method.

Teble 10. Preliminarily result of surface gravity (LOGG) for 5 stars calculated with spectral lines.

Star	Teff	logg	Fe/H	ξ_t	"LOGG 1 pre."
HD28185	5667	4.42	0.21	0.94	4.31
HD28254	5653	4.15	0.36	1.08	4.20
HD28471	5745	4.37	-0.05	0.95	4.11
HD28701	5710	4.41	-0.32	0.95	3.9
HD29137	5768	4.28	0.3	1.1	4.18

The discrepancies in our preliminary result can be caused by the two fixed parameters, metallicity and microturbulence velocity, and normalization of the observed spectra for finding WD.

5. Testing the Grid

We know that the line profiles are affected by many parameters: effective temperature, surface gravity, microturbulence velocity, metallicity. Our first grid only contains the effective temperature and surface gravity. We need to check also the dependence of the other above mentioned main parameters (ξ_t, [X/H]).

5.1. Effect of the microturbulence velocity

As mentioned before we have fixed two parameters: metallicity and microturbulence velocity.

We need to compute synthetic spectra to fill the grid of data for further determinations of spectroscopic surface gravity. To get synthetic spectra we used MOOG, as described before. Synthetic spectra were computed with changing the effective temperature and the surface gravity. For more accuracy we also need to change the other parameters, i.e. metallicity, microturbulence velocity, and rotational velocity.

The synthetic spectra was also computed for different microturbulence velocity from 0.5 to 2.0 with 0.5 steps for a fixed temperature, metallicity and surface gravity (T=5700 K, [Fe/H]=0.0 dex and logg=4.50 dex). This will give us an idea how the microturbulence velocity acts on the synthetic spectra.

To check how much the synthetic spectra is changing with different microturbulence velocity we plot the synthetic spectra for different value of microturbulence velocity.

The changes of microturbulence velocity does not have big impact on the line profile of the synthetic spectrum as can be seen in the Figure 9.

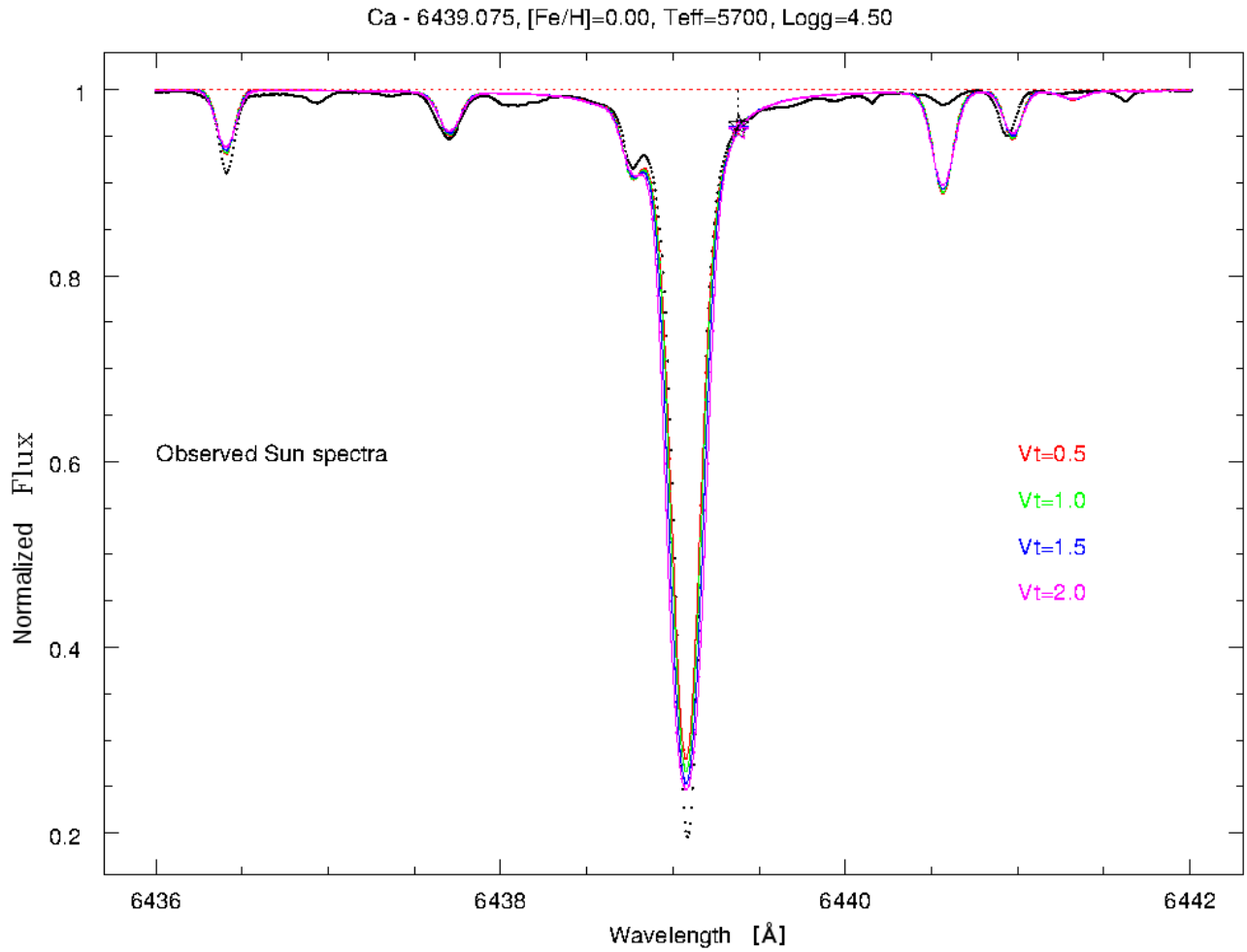

Figure 9. Black dots correspond to the observed Sun spectra. Central line is a CaI line at 6439.08 Å. Colored lines correspond to the synthetic spectrum with different microturbulence velocity. Stars-like symbols correspond to the average point and vertical dashed black line corresponds to the value of WD.

Because the changes in microturbulence velocity does not have a strong impact on the synthetic spectra, we will keep it fixed as was done before: Vt=1.0.

The surface gravity derived for star with T_{eff} = 5700 K, logg = 4.50 dex, and [Fe/H] = 0.0 dex parameters for different microturbulence velocity is given in Table 11.

Table 11. Surface gravity derived for same sample star with different microturbulence velocity.

ξ_t (km/s)	WD (6439.08)	Logg(6439.08) (dex)
0.5	0.04279	4.49
1.0	0.04305	4.50
1.5	0.04352	4.51
2.0	0.04424	4.52
		sigma = 0.01

As can be seen in Table 11 the results derived by each line are very close to the initial surface gravity of sample star and on average the difference between initial and derived surface gravity is 0.01 dex.

5.2. Limitation on the Rotational velocity

In our calculation we have a limitation on the rotational velocity. We know that the spectral lines of high rotating stars are wider than in a slow rotating star.

A star that is rotating will produce a Doppler shift (Figure 10) in each line of the star's spectrum. The amount of broadening depends on rotation rate and the angle of inclination of the axis of rotation to the line of sight. Astrophysicists can use this effect to calculate the stellar rotation rate. For simplicity lets assume that the axis of rotation is perpendicular to the line of sight of the observer. If the change in wavelength of a line at wavelength λ is Δλ then the velocity v of atoms on the limb of a rotating star is given by:

$$v = c\frac{\Delta\lambda}{\lambda}$$

Astrophysicists have found that, in general, the hottest stars (type O and B) rotate the fastest with periods reaching only 4 hours. G-type stars like the sun rotate fairly slowly at about once every 27 days.

The effects of rotation on the continuous spectrum are small except when rotation is very near the break-up rate. The spectral lines, on the other hand, are strongly changed by the relative Doppler shifts of the light coming from different parts of the stellar disk.

The Doppler line broadening from rotation depends on the orientation of the axis of rotation relative to the line of sight.

The shape of most photospheric spectral lines is basically the shape of the Doppler-shift distribution, i.e., the fraction of starlight at each Doppler shift. Essentially every element of surface from which light comes to us is moving relative to the center of mass of the star. The motions arise primarily from photospheric velocities such as granulation and oscillations, and from rotation of the star. The line-of-sight components of these velocities, integrated over the apparent disk of the star, is the Doppler-shift distribution.

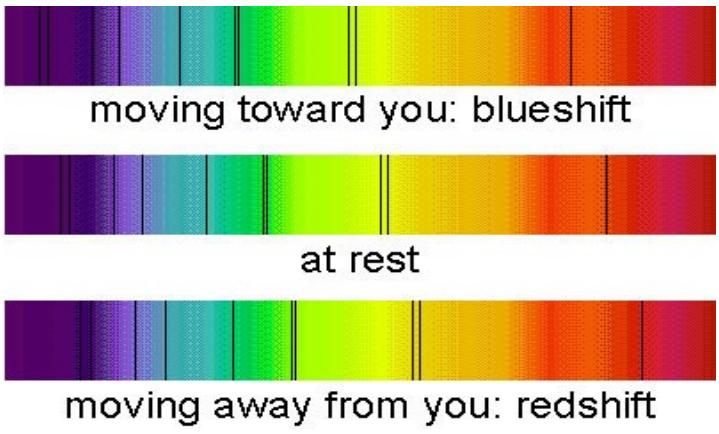

Figure 10. Doppler-Shift. Black vertical lines corresponds to the absorption lines in the spectra, and the colors represent different wavelength ranges.

To take into account this fact and understand the changes we made a plot of synthetic spectra for different value of the rotational velocity (Figure 11).

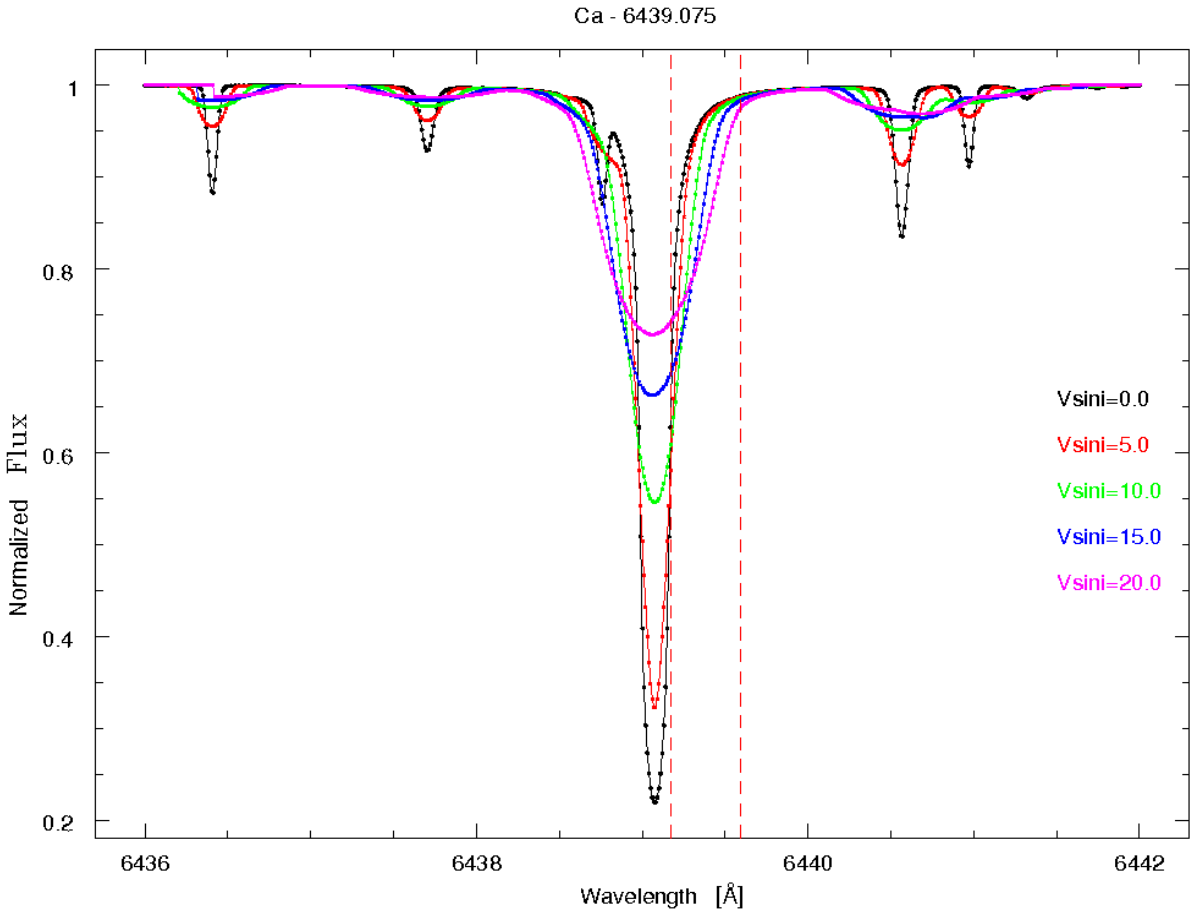

Figure 11. Black dotes corresponding to the observed spectra and colored lines corresponding to the synthetic spectra for different value of rotational velocity. Red vertical lines present the «stable» region of spectrum.

In Figure 11 we present the synthetic spectra for different value of *vsini* form 0.0 km/s to 20.0 km/s with 5.0 km/s step. The black spectrum corresponding to the observed Sun spectra in a wavelength range at 6436.00 Å – 6442.00 Å. The colored lines corresponding to the synthetic spectrum for different value of *vsini*. As can be seen in the Figure 11 the most «stable» part of spectra, which is presented with vertical red dashed lines, is changing with *vsini*. The changes of the rotational velocity up to 7 km/s does not produce too much wideness of the spectra, but for higher value of *vsini* makes spectra wider and the changes in the «stable» region are too much. This was a reason to put a limitation on the rotational velocity. The further calculation were done taking into account limitation on *vsini* not more than 7 km/s. Our calculations valid within the 7 km/s and bigger values for *vsini* will make significant discrepancies in our calculations.

The surface gravity derived for different rotational velocity for same sample star as was done for different microturbulence velocity is given in Table 12.

Table 12. Surface gravity derived for same sample star with different rotational velocity.

vsini (km/s)	WD (6439.08)	Logg(6439.08) (dex)
0.0	0.04305	4.50
5.0	0.04823	4.59
7.0	0.05585	4.72
10.0	0.07772	Out of range
15.0	0.14213	Out of range
20.0	0.1789	Out of range
		Sigma = 0.14

As can be seen in Table 12 the results derived by each line are close to the initial surface gravity for lower values of *vsini*, with increasing the value of rotational velocity our calculation is out of range.

On average the difference between initial and derived surface gravity is 0.14 dex. For higher values of v*sini* we should recalculate and rebuild our grid.

6. Improving the Grid

6.1. Distribution of elemental abundances

Metallicity determination is an important part of a complete spectroscopic characterization of a star. We now know that stars are mostly made up of hydrogen and helium, with small amounts of some other elements. Metallicity is given by the ratio of the amount of one chemical element to the amount of the Hydrogen: [X/H]. Usually we use the Iron: [Fe/H].

Laboratory experiments on Earth showed that different elements have different spectroscopic signature. Astrophysics takes advantage of these techniques for the study of the chemical composition in stars. Modern spectroscopy is highly efficient and is often conducted with very high resolution spectrographs that show spectral lines in fine detail.

The presence of a spectral line corresponds to a specific energy transition for an ion, atom or molecule in the spectrum of a star indicates that the specific ion, atom or molecule is present in that star. This was how helium was first discovered in the Sun before it was isolated on Earth.

However, we should notice that we are once more limited by: 1) the fact that we do not have access to the star's core, and 2) we are only able to determine relative amount of different elements. And 3) the absence of a spectral line does not necessarily mean that the element does not exist.

Astronomers can not only detect the presence of a line but they are often able to determine the relative amounts of different elements and molecules present. They can thus determine the metallicity of a star.

To know how synthetic spectra changes with metallicity, as we study Ca, Na and Mg lines for determination of stellar surface gravity, we need to change in the program [Ca/H], [Mg/H] and [Na/H]. The ratio of mentioned elements we found from the [Fe/H] vs [X/H] relation (Figure 12).

The sample used to determine the [X/H] versus [Fe/H] consists of 1111 FGK stars observed within the context of the HARPS GTO (Guaranteed Time Observation) programs. It is a combination of three HARPS sub-samples: HARPS-1 (Mayor et al. 2003), HARPS-2 (Lo Curto et al. 2010) and HARPS-4 (Santos et al. 2011).

The stars are slowly-rotating and non-evolved solar-type dwarfs with spectral type between F2 and M0 which also do not show high level of chromospheric activity.

Elemental abundances for 12 elements (Na, Mg, Al, Si, Ca,Ti, Cr, Ni, Co, Sc, Mn and V) have been determined in Adibekyan et al. (2012) work using a local thermodynamic equilibrium (LTE)

analysis with the Sun as reference point with the 2010 revised version of the spectral synthesis code MOOG (Sneden 1973) and a grid of Kurucz ATLAS9 plane-parallel model atmospheres (Kurucz et al. 1993). The reference abundances used in the abundance analysis were taken from Anders & Grevesse (1989).

The data were take from Adibekyan et al. (2012) work to determine the [X/H] vs [Fe/H] ratio.

The dependence is approximately linear as can be seen in Figure 12 and the fit was done according to the equation (11).

$$\begin{aligned}[Ca/H] &= 0.024857 + 0.754988 \times [Fe/H] \\ [Na/H] &= 0.038687 + 1.035518 \times [Fe/H] \\ [Mg/H] &= 0.019539 + 0.791280 \times [Fe/H]\end{aligned} \qquad (11)$$

The coefficients were determined according to the second order of polynomial fit.

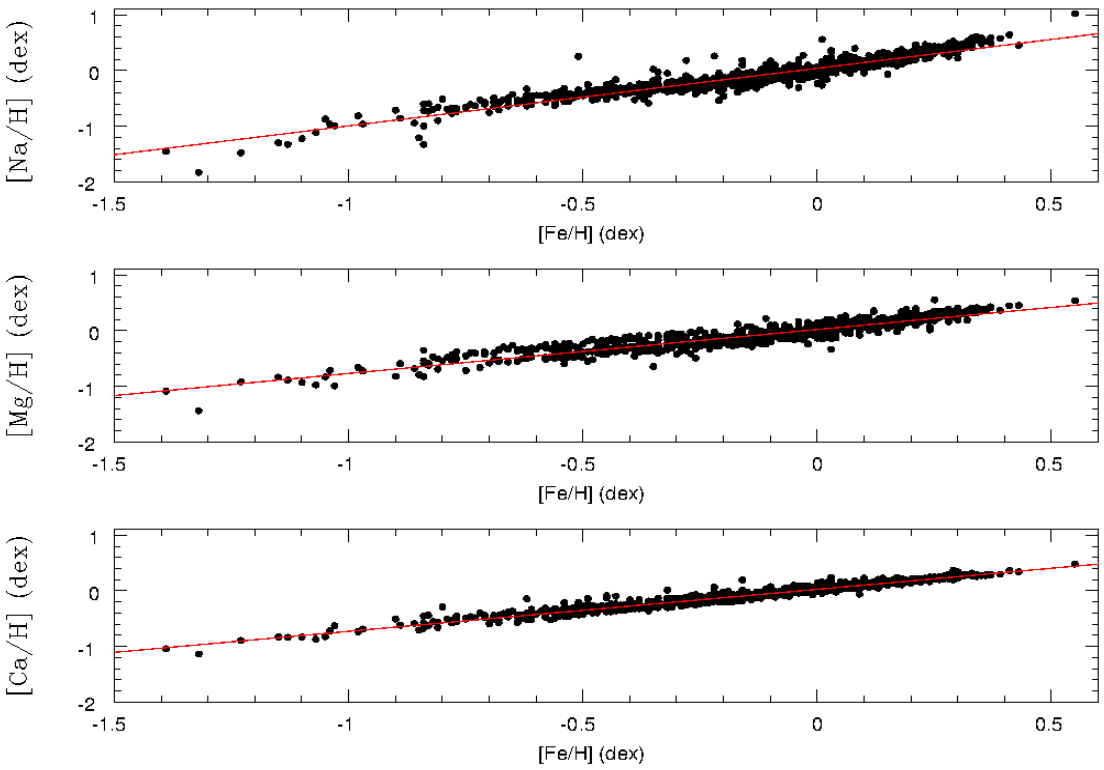

Figure 12. [Ca/H], [Mg/H], and [Na/H] versus [Fe/H] from bottom to top respectively. Black dots corresponding to the 1111 stars. Red line corresponding to the linear fit.

We determine the abundances of the Ca, Na, and Mg elements with equation (11). As we used Ca, Na, and Mg lines in our calculations we need to take into account the initial value of each element. The initial value of abundances of each element is given in Table 13.

6.2. Metallicity term

Moving forward we need to take into account the contribution of metallicity in the shape of synthetic spectra. We created the grid of abundances of the elements corresponding to the certain value of [Fe/H] from -1.5 to 0.5 with steps 0.25 to use in a MOOG for computing synthetic spectra (Table 14). The grid was made by interpolation following to the distribution of elements in our sample.

Table 13. The abundances of elements corresponding to the certain value of [Fe/H]

[Fe/H]	[Ca/H]	[Mg/H]	[Na/H]
-1.5	-1.11	-1.17	-1.51
-1.25	-0.92	-0.97	-1.26
-1.0	-0.73	-0.77	-0.99
-0.75	-0.54	-0.57	-0.74
-0.5	-0.35	-0.38	-0.48
-0.25	-0.16	-0.18	-0.22
0.0	0.02	0.02	0.04
0.25	0.21	0.22	0.29
0.5	0.40	0.42	0.56

Taking into account all this conditions, we computed synthetic spectra with MOOG for different values of effective temperature, metallicity and surface gravity to create the grid of parameters for further calculations. We calculated the value of WD with the same technique which was described before, and made a «models» with different metallicity (for each value of [X/H]) and effective temperature, which contain the value of surface gravity between 1.0 to 5.0 and corresponding value of WD.

The input parameters in our code are Teff, [Fe/H], and WD. Our grid has a certain value of effective temperature and metallicity. The input parameters not always can be certain value from our range of grid, and for that the interpolation was done to find final value of surface gravity. We are taking the nearest «models» of our input parameters and with the interpolation we find surface gravity of stars.

With two fixed parameters interpolation was done with taking two «models» related to the effective temperature, but in this case we have to take into account also metallicity. And for interpolation now we have four «models» related to the effective temperature and metallicity instead of two. At first interpolation was done between «models» related to the effective temperature for same value of metallicity (Figure 13. 1 «M» and 2 «M») associated to the previous and next values of the effective temperature and was found «model» for corresponding input effective temperature for one value of metallicity («1 interpol.»). Then the second pair of «models» were taken for interpolation (3 «M» and 4 «M») and middle «model» have been found («2 interpol.»). After, the interpolation was done between two found «models» with first two interpolations («3 interpol.»). The schematic representation of interpolation is shown in a Figure 13.

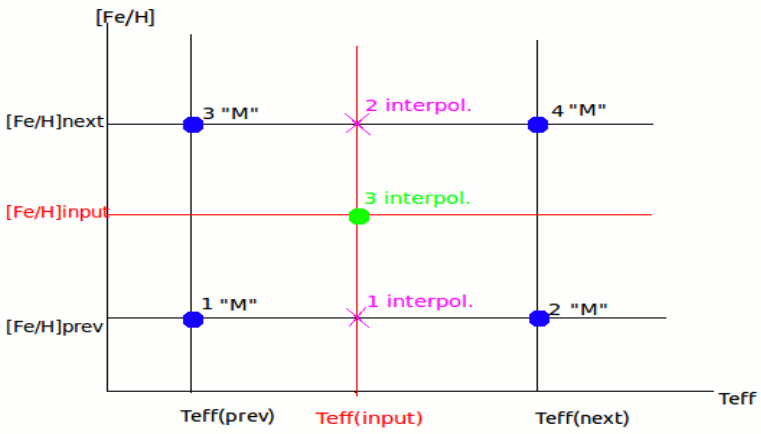

Figure 13. The schematic representation of the interpolation. 1 «M», 2 «M», 3 «M» and 4 «M» corresponding to the 1, 2, 3 and 4 «models» respectively. 1 interpol. is the middle «model» found by interpolating 1 «M» and 2 «M». 2 interpol. is the same for second pair of «models». 3 interpol. is the result of the interpolation of middle «models», i.e. interpolation of the 1 interpol. and 2 interpol.

The 3 interpol. is the final result of interpolation and final grid of our parameters.

So, for a given effective temperature and given metallicity in range between 4500-6500 K and -1.5-0.5 dex respectively, we are able to find the surface gravity of stars in a range 1.0 - 5.0 dex. The code is available in electronic version in the CD.

7. Discussion and Conclusion

We have studied the Ca, Na, and Mg lines which are extremely sensitive to the surface gravity for a fast estimation of the stellar surface gravity. Those lines were used in Bruntt el al. (2010) work to determine the surface gravity (*logg*) by using synthesis method.

They found that the Mg I b line in CoRoT-7 is not very sensitive and give lower values than the Ca lines. The reason may be the high degree of blending with weaker lines for such a late type stars. And also they neglect the results for the Mg I b lines since the higher value of logg was in good agreement with the result using Fe I and Fe II lines.

In our work we study eight spectral lines given in Table 1. We used spectral synthesis method to make a grid of parameters which will give us an information about surface gravity. The grid was made for different values of effective temperature from 4500K to 6500K, and metallicity from -1.5 dex to 0.5 dex. As was described before in section 5.1, microturbulence velocity does not have too much impact on the shape of the spectral lines. We kept the microturbulence velocity equal to 1.0. We discussed also the role of the rotational velocity in section 5.2 and put a limitation on vsini.

In terms of metallicity, we took into account the abundances of Ca, Na and Mg. The abundances were determined from [X/H] vs [Fe/H] ratio. Corresponding values were used in MOOG for computation of synthetic data.

We have a complete grid of data for the determination of the stellar surface gravity. In Figure 14 we shown Ca, Na, and Mg lines in a solar spectra.

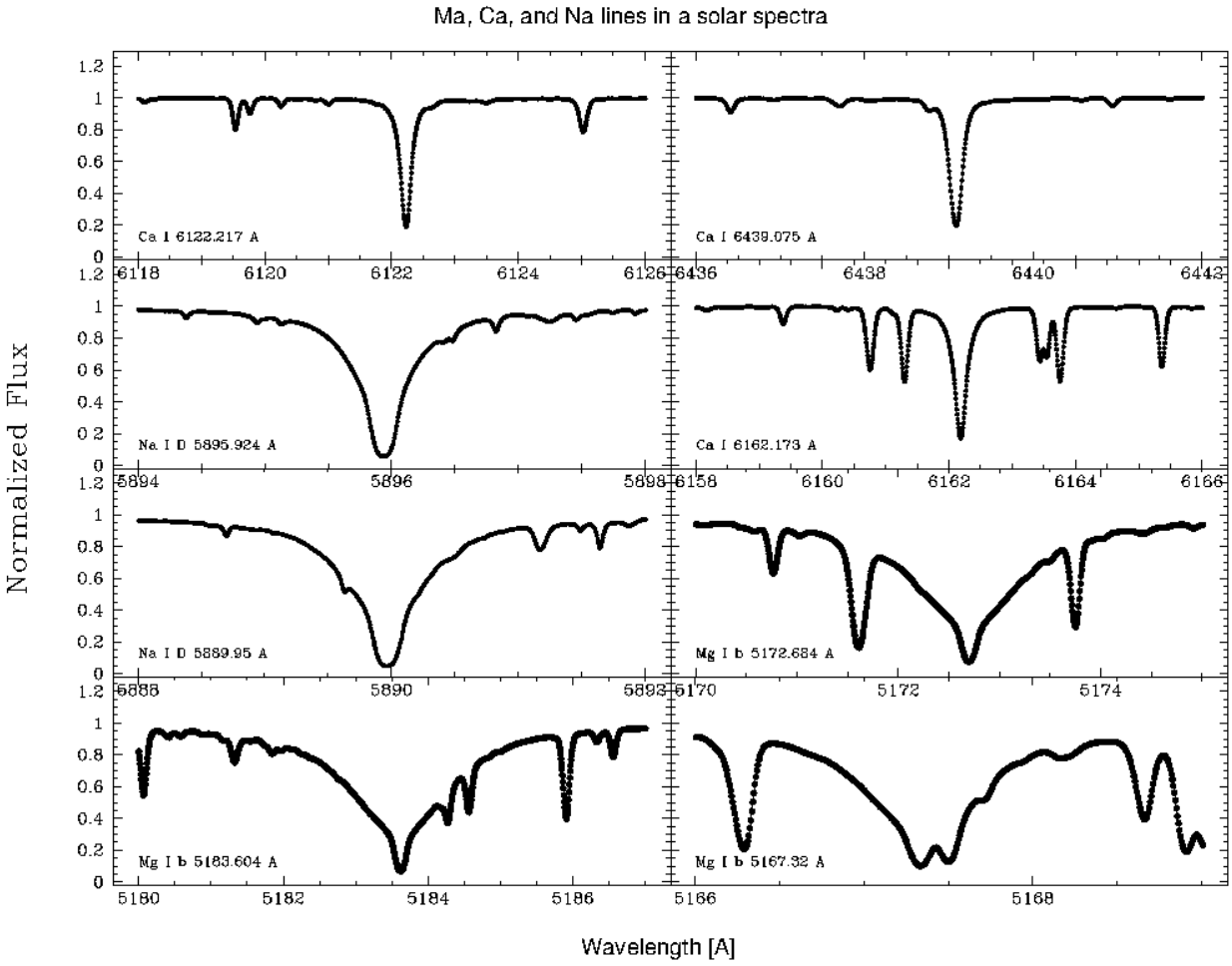

Figure 14. Spectral lines in a solar spectra. The element and corresponding wavelength written in each box left-bottom side.

As can be seen in a Figure 14, Mg I b lines are too blended. For our calculations we chose isolated lines, i.e. Ca I lines at 6439.08 Å and 6122.21 Å, to avoid the blending with nearest weak lines. For six of this eight lines we can use another approach to determine atmospheric parameters, e.g. spectral synthesis method.

For the determination of WD according to the equation (10) we need to have a spectrum normalized to one in a given region of wavelength. For normalization we used a subroutine from the ARES code[3].

3 http://www.astro.up.pt/~sousasag/ares/

7.1. Testing

Knowing the effective temperature, metallicity and WD parameter we can estimate the surface gravity of stars using our grid.

The test was done for 150 slow rotating (not more than 7 km/s) stars from HARPS GTO program. Effective temperature range of our choice lie from about 4600 to 6800 K, metallicity ranges from -0.7 to 0.3 dex, and surface gravity - from about 3.6 to 4.9 dex. The table of the stars with atmospheric parameters are given in appendix 1.

With our method we were able to determine surface gravity of 89 stars out of 150 (appendix 2).

The automatic normalization of 61 stars out of 150 is not good. It can be a reason of blended lines near the central line.

The results determined for 89 stars from two Ca I lines at 6439.08 Å and 6122.21 Å are given in Table 14. Full table is given in appendix 2. In the table first column correspond to the name of the star, second and third columns correspond to the value of surface gravity determined by Ca I lines. Fourth column correspond to the average value of the logg and fifth column is the half of the difference of *logg* values determined by each line.

Sigma is a half of the difference between two values for logg defined from each Ca I line and not a standard deviation (σ). Unfortunately we did not have more than two lines to determine surface gravity.

Table 14. Surface gravity of stars derived by our method.

Star	logg(6439.08)	logg(6122.21)	Average logg	sigma	logg Sousa
HD21938	3.9683	3.72584	3.84707	0.12	4.38
HD21019	3.34854	3.29253	3.320535	0.03	3.93
HD27471	4.20873	4.17637	4.19255	0.02	4.25
HD19423	4.14979	4.08387	4.11683	0.03	4.23
HD21161	4.35926	4.38318	4.37122	0.01	4.24
...	...	...	...	...	...
...	...	...	...	...	...
HD192310	4.76812	4.5756	4.67186	0.09	4.51
HD195564	4.23735	4.08209	4.15972	0.08	4.03
HD198075	4.43672	4.23499	4.335855	0.1	4.56

We also made a comparison between our result and before determined result by other authors. The comparison plot between our results and Sousa et al. (2011) results is shown in Figure 15.

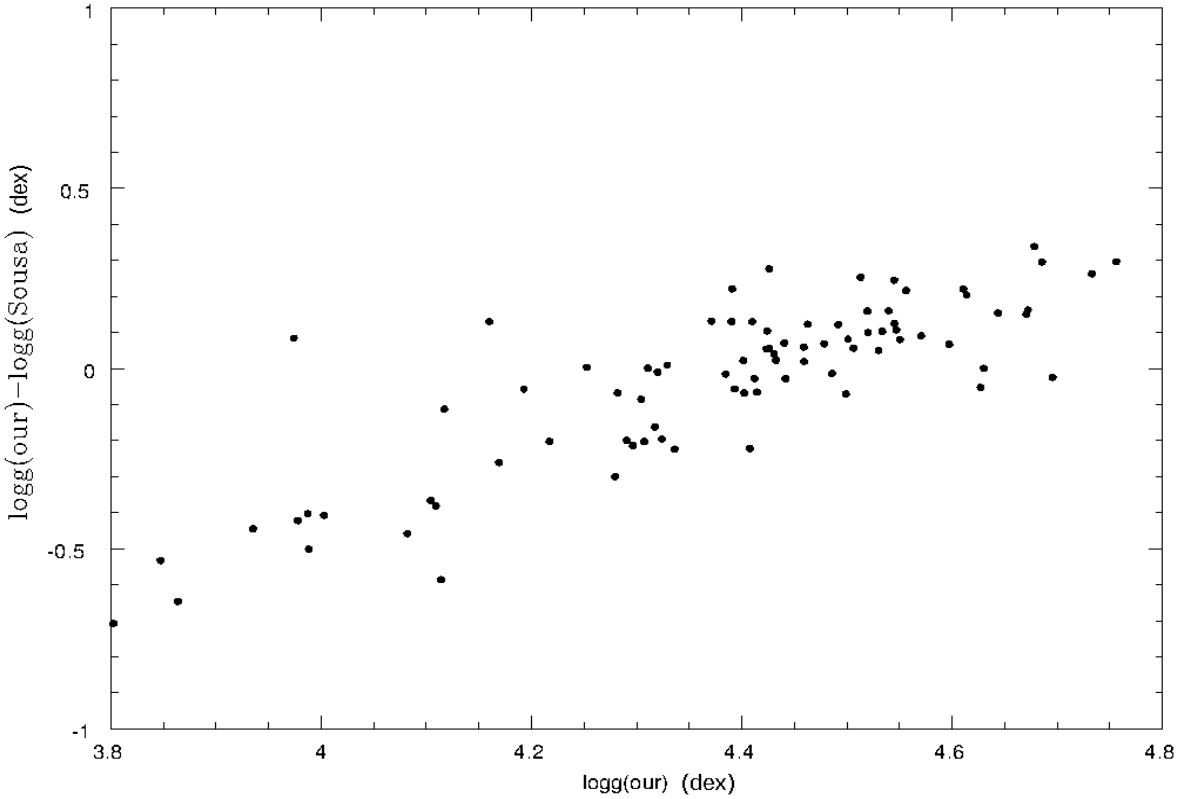

Figure 15. Comparison between Sousa et al. (2011) results and our results.

From Geneva-Copenhagen survey re-analysis catalog we could extract parameters only for 52 stars from our choice. We also compared our results with Casagrande et al. (2011) work. The comparison plot is shown in Figure 16.

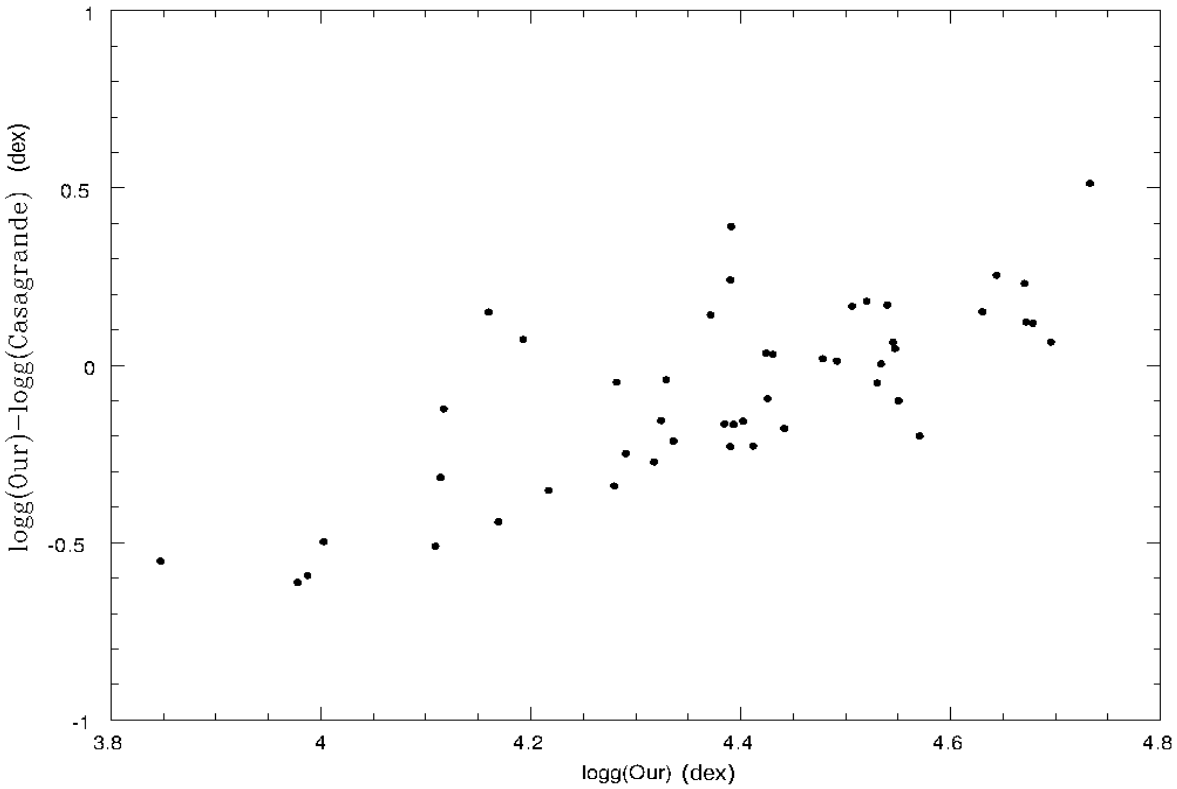

Figure 16. Comparison of our results and Casagrande et al. (2011) results.

As can be seen in Fig. 15 and Fig. 16 our results are good for dwarfs, but for stars with low surface gravity we have discrepancies. We also made a histogram to see the distribution of the points (Figure 17). The size of each bin is 0.1 dex. As can be seen in Fig. 17 the peak is around 0, which means that our results are not far from the correct values.

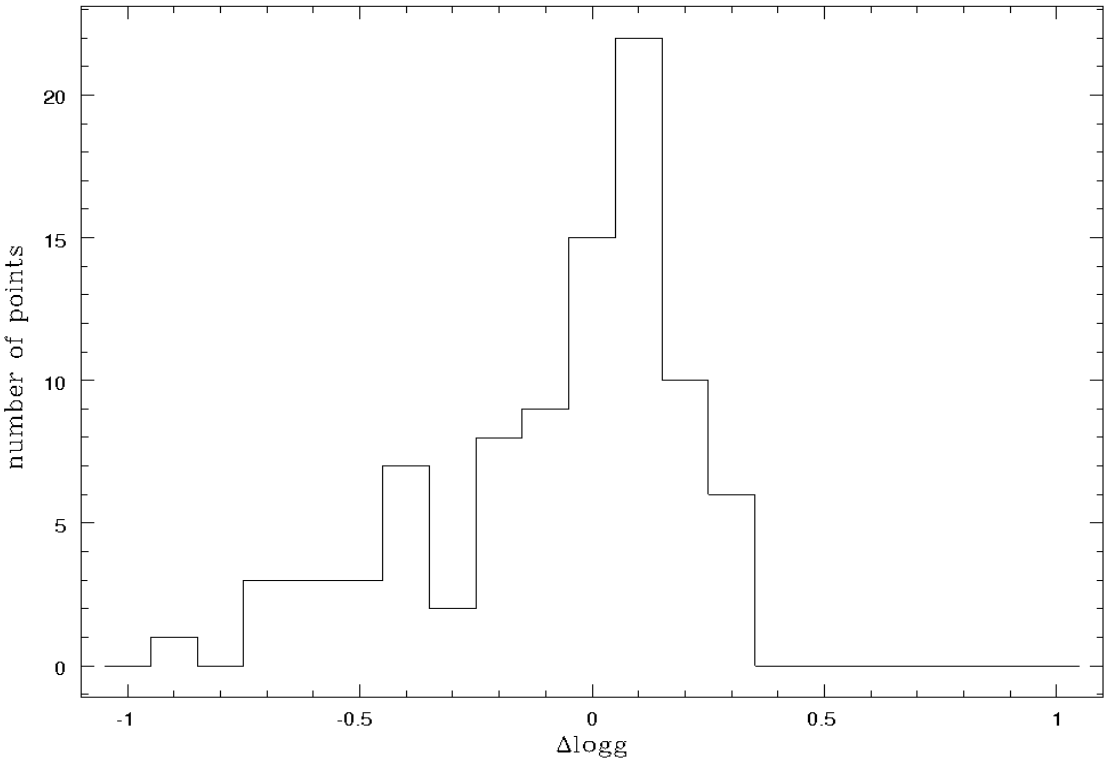

Figure 17. The distribution of the number of points.

To understand this discrepancies we made a plot of the difference of the *logg*'s values versus other parameters, such as effective temperature, metallicity and microturbulence (Figure 18)

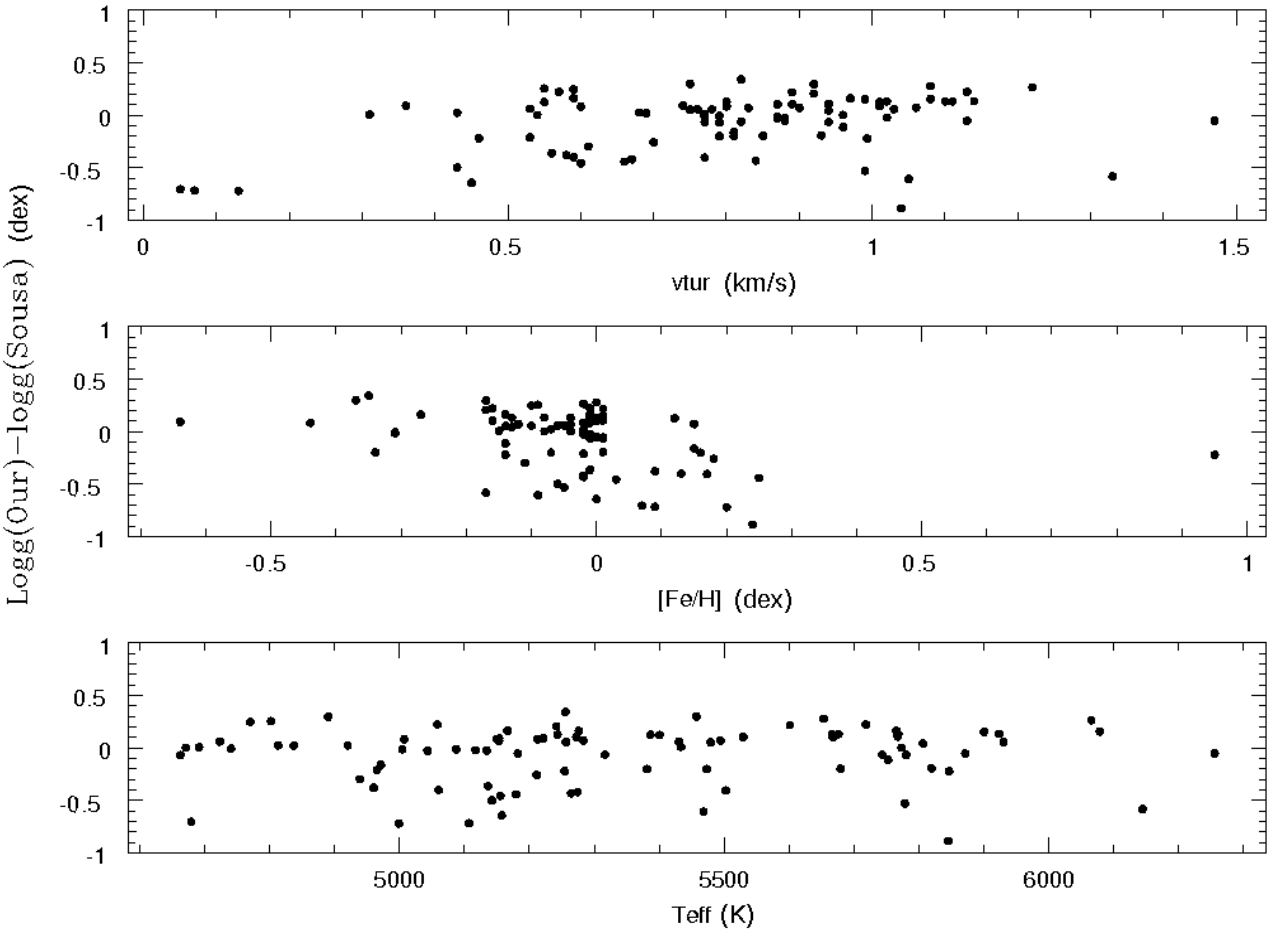

Figure 18. Comparison plot of Δlogg versus microturbulence velocity, metallicity, and effective temperature from top to bottom, respectively.

As can be seen in Figure 18 there is no clear dependence between *Δlogg* and other parameters.

In the future it would be interesting to find the solution of this problems. We should be then study the lines more to understand the reason for the discrepancies.

7.2. Conclusion

We have describe the VALD from where were extracted line lists for computation of synthetic spectra. Also we adjusted Van der Waals parameter which has an important effect on the shape of lines, and we presented the table for adjusted Van der Waals parameter for each line. The description of MOOG was presented with necessary input parameters also description of model atmosphere, SYNTH driver which we used to compute synthetic spectra for making a grid of data.

We presented a method to estimate the stellar surface gravity using spectral lines which are extremely sensitive to the surface gravity. We have also presented the method for determination for the Van der Waals parameter according to the χ^2 minimization. The part of the wing of the spectra were selected by looking at the spectra for different values of effective temperature (5000K, 5700K, 6200K, 6500K) and surface gravity (2.0, 3.0, 4.44, 5.0). The most «stable» part of the synthetic spectra was selected to perform χ^2 minimization. In the Table 9 we bring the «stable» part of wings of synthetic spectra for all eight lines.

We presented the quantity WD which was computed from the normalized spectra. The grid was made for every line corresponding «stable» part of wing of spectra and corresponding wavelength of average point. Also 3D distribution of the WD was presented in Figure 8.

A preliminary test was performed for 5 stars with effective temperature from 5600 to 5800 K, microturbulence velocity close to one and metallicity close to solar metallicity.

The code was improved for more accurate results taking into account the metallicity and microturbulence velocity terms. We completed the grid for determination of surface gravity including parameters. We also showed that the changes in microturbulence velocity does not act on the synthetic spectra and we can keep it fixed. In case of metallicity, we took into account the [X/H] versus [Fe/H] ratio and found the corresponding value of abundances of our elements and used in the code. The data for [X/H] vs [Fe/H] were taken from HARPS GTO program which contain 1111 FGK stars.

We also took into account that the spectral lines for higher rotating stars are wider. The synthetic spectra was computed for different rotational velocity and we have put the limitation on the rotational velocity. Our calculations seems to be valid within the 7 km/s. For higher value of v*sini* we should recalculate and rebuild our grid.

The test was done for 150 stars from HARPS GTO program. The final results were determined for 89 stars which were in range of our determination limit. The other stars 61 out of 150 was out of grid. We also compare our results with results derived by Sousa et al. (2011) and Casagrande et al.

(2011). From the plots we can see that our results are reasonable for dwarf stars and we have discrepancies for stars with lower surface gravity. The comparison plot which was made to understand probable reason of the discrepancies shows no clear dependence between Δlogg and effective temperature, metallicity, and microturbulence velocity.

In future we are planning to study the lines more carefully to understand which parameters can be the reason for the discrepancies.

References

Adibekyan, V. Zh.; Sousa, S. G.; Santos, N. C.; Delgado Mena, E.; Gonzalez Hernandez, J. I.; Israelian, G.; Mayor, M.; Khachatryan, G. 2012arXiv1207.2388A

Anders, E., & Grevesse, N. 1989, Geochim. Cosmochim. Acta, 53, 1973

Bruntt, H.; Deleuil, M.; Fridlund, M.; Alonso, R.; Bouchy, F.; Hatzes, A.; Mayor, M.; Moutou, C.; Queloz, D. 2010A&A...519A..51B

Casagrande, L.; Schoenrich, R.; Asplund, M.; Cassisi, S.; Ramirez, I.; Melendez, J.; Bensby, T.; Feltzing, S. 2011yCat..35309138C

Cayrel, Giusa; Cayrel, Roger 1963ApJ...137..431C

Cayrel de Strobel, G. 1969, Theory and observation of normal stellar atmospheres, ed. O. Gingerich 1969tons.conf.....G

Drake, Jeremy J.; Smith, Geoffrey 1991MNRAS.250...89D

Drake, Jeremy J.; Smith, Geoffrey 1993ApJ...412..797D

Edmonds, F. N., Jr. 1969JQSRT...9.1427E

Edvardsson, B. 1988a, The impact of very high S/N spectroscopy on stellar physics, Cayrel de Strobel, G.; Spite, Monique 1988IAUS..132.....C

Edvardsson, B. 1988A&A...190..148E

Ekberg J.O., 1997, Phys. Scr. 56, 141

Fuhrmann, K.; Pfeiffer, M.; Frank, C.; Reetz, J.; Gehren, T. 1997A&A...323..909F

Gray, D. F. 1992oasp.book.....G

Gray, D. F. 2004AdSpR..34..308G

Gray, D. F. 2008oasp.book.....G

Gray, David F.; Brown, Kevin 2001PASP..113..723G

Gray, David F.; Johanson, Heather L. 1991PASP..103..439G

Kovtyukh, V. V.; Soubiran, C.; Belik, S. I.; Gorlova, N. I. 2003A&A...411..559K

Kurucz, Robert 1993KurCD..13.....K

Kupka, F.; Piskunov, N.; Ryabchikova, T. A.; Stempels, H. C.; Weiss, W. W. 1999A&AS..138..119K

Lo Curto, G., Mayor, M., Benz, W., et al. 2010, A&A, 512, A48

Mayor, M., Pepe, F., Queloz, D., et al. 2003, The Messenger, 114, 20

Piskunov, N. E.; Kupka, F.;Ryabchikova,T.A.;Weiss,W.W.;Jeffery,C.S. 1995A&AS..112..525P

Santos, N. C., Mayor, M., Bonfils, X., et al. 2011, A&A, 526, 112

Smith, G.; Edvardsson, B.; Frisk, U. 1986A&A...165..126S

Smith, G.; Drake, J. J. 1987A&A...181..103S

Smith, G.; Lambert, D. L.; Ruck, M. J. 1992A&A...263..249S

Sneden, C. 1973, Ph.D. Thesis, Univ. of Texas

Sneden, C. 2002 http://www.as.utexas.edu/~chris/codes/WRITEMOOG.ps

Sousa, S. G.; Santos, N. C.; Mayor, M.; Udry, S.; Casagrande, L.; Israelian, G.; Pepe, F.; Queloz, D.; Monteiro, M. J. P. F. G. 2008yCat..34870373S

Sousa, S. G.; Alapini, A.; Israelian, G.; Santos, N. C. 2010A&A...512A..13S

Sousa, S. G.; Santos, N. C.; Israelian, G.; Mayor, M.; Udry, S. 2011A&A...533A.141S

Strassmeier, K. G.; Schordan, P. 2000AN....321..277S

Unsöld, A. 1955. Physik der Sternatmosphären, 2nd edn. (Berlin: Springer-Verlag), pp. 326, 331.

Appendix 1. Table of all tested stars with atmospheric parameters.

Star	T_{eff}	Logg	[Fe/H]	ξ_t
HD10002	5313	4.4	-0.69	0.82
HD10166	5221	4.48	-0.64	0.74
HD10180	5911	4.39	-0.64	1.11
HD10700	5310	4.44	-0.56	0.55
HD11226	6098	4.35	-0.51	1.28
HD11505	5752	4.38	-0.46	0.99
HD11683	5007	4.42	-0.44	0.6
HD11964A	5332	3.9	-0.41	0.99
HD12345	5395	4.44	-0.4	0.69
HD12387	5700	4.39	-0.39	0.93
HD12617	4890	4.46	-0.37	0.75
HD13060	5255	4.34	-0.35	0.82
HD1320	5679	4.49	-0.34	0.85
HD13724	5868	4.52	-0.31	1.02
HD13789	4740	4.33	-0.31	0.79
HD13808	5087	4.4	-0.31	0.77
HD1388	5954	4.41	-0.31	1.13
HD14374	5425	4.48	-0.29	0.81
HD1461	5765	4.38	-0.27	0.97
HD1581	5977	4.51	-0.22	1.12
HD18083	6144	4.7	-0.17	1.33
HD18386	5457	4.39	-0.17	0.92
HD18719	5241	4.41	-0.17	0.92
HD18777	5058	4.39	-0.16	0.57
HD18822	5272	4.43	-0.16	0.87
HD18838	5500	4.48	-0.16	0.64
HD19034	5477	4.4	-0.16	0.69
HD19230	5254	4.63	-0.14	0.46
HD19423	5752	4.23	-0.14	0.96
HD19467	5720	4.31	-0.14	0.96

HD19641	5806	4.39	-0.13	0.94
HD199086	6149	4.65	-0.12	1.21
HD19994	6289	4.48	-0.12	1.72
HD20003	5494	4.41	-0.12	0.83
HD2025	4939	4.58	-0.11	0.61
HD202819	4737	4.4	-0.11	0.59
HD20407	5866	4.5	-0.1	1.09
HD20492	4770	4.3	-0.1	0.59
HD20619	5703	4.51	-0.1	0.92
HD207129	5937	4.49	-0.1	1.06
HD20781	5256	4.37	-0.1	0.78
HD20782	5774	4.37	-0.09	1
HD20794	5401	4.4	-0.09	0.67
HD20807	5866	4.52	-0.09	1.04
HD20852	6813	4.76	-0.09	2.34
HD20868	4802	4.26	-0.09	0.55
HD21019	5468	3.93	-0.09	1.05
HD21132	6243	4.6	-0.08	1.44
HD21161	5923	4.24	-0.08	1.14
HD21209A	4671	4.31	-0.08	0.54
HD21251	4920	4.41	-0.07	0.68
HD21411	5473	4.51	-0.07	0.81
HD21693	5430	4.37	-0.06	0.76
HD21749	4723	4.4	-0.06	0.53
HD21759	5142	4.49	-0.06	0.43
HD21938	5778	4.38	-0.05	0.99
HD21977	5930	4.45	-0.05	1.03
HD22049	5153	4.53	-0.04	0.9
HD22177	5666	4.26	-0.04	1.02
HD22249	5773	4.63	-0.04	0.96
HD22282	5433	4.32	-0.04	0.77
HD225297	6181	4.55	-0.02	1.24
HD22610	5043	4.44	-0.02	0.88
HD22879	5884	4.52	-0.02	1.2

HD22897	4837	4.44	-0.02	0.69
HD22918	4924	3.61	-0.02	0.73
HD23030	5951	4.37	-0.02	1.22
HD23079	5980	4.48	-0.02	1.12
HD23249	5150	3.89	-0.02	1.01
HD23356	5004	4.5	-0.02	0.87
HD23456	6178	4.56	-0.02	1.38
HD23472	4813	4.38	-0.02	0.43
HD23901	5264	3.93	-0.02	0.84
HD24062	6107	4.62	-0.02	1.34
HD24085	6065	4.47	-0.02	1.22
HD24112	6175	4.35	-0.02	1.26
HD24331	4965	4.51	-0.02	0.53
HD24558	5274	4.4	-0.02	0.67
HD24633	5276	4.36	-0.01	0.59
HD24892	5363	3.99	-0.01	0.88
HD25061	5243	4.42	-0.01	0.8
HD25105	5316	4.47	-0.01	0.77
HD25120	5134	4.47	-0.01	0.87
HD25171	6160	4.43	-0.01	1.22
HD25357	5117	4.72	-0.01	1.02
HD25565	5212	4.47	-0.01	0.8
HD25587	6258	4.61	-0.01	1.78
HD25673	5136	4.47	-0.01	0.56
HD25704	5942	4.52	-0.01	1.37
HD25912	5900	4.52	-0.01	0.99
HD26430	4948	4.37	-0.01	0.55
HD26729	5718	4.17	-0.01	1.13
HD26887	6016	4.46	-0.01	1
HD26965A	5153	4.39	-0.01	0.36
HD27063	5767	4.44	-0.01	0.94
HD27471	5871	4.25	-0.01	1.13
HD27894	4952	4.39	-0.01	0.78
HD28185	5667	4.42	0	0.94

HD28254	5653	4.15	0	1.08
HD283	5157	4.51	0	0.45
HD28471	5745	4.37	0	0.95
HD28701	5710	4.41	0	0.95
HD28807	6602	4.67	0	1.89
HD28821	5660	4.38	0	0.88
HD28969	6255	4.68	0	1.47
HD29137	5768	4.28	0	1.1
HD29263	5780	4.35	0.01	0.94
HD29303	5819	4.52	0.01	0.93
HD29428	5743	4.48	0.01	0.82
HD29980	6019	4.71	0.01	1.57
HD29985	4678	4.39	0.01	0.65
HD30053	6139	4.51	0.01	1.2
HD30177	5601	4.34	0.01	0.89
HD30278	5394	4.39	0.01	0.72
HD30306	5529	4.32	0.01	0.89
HD30523	4662	4.57	0.01	0.79
HD30669	5400	4.37	0.01	0.55
HD30858	5182	4.45	0.01	0.88
HD31103	6078	4.49	0.01	1.08
HD31128	6096	4.9	0.01	3.02
HD3569	5155	4.54	0.03	0.6
HD36108	5916	4.33	0.03	1.21
HD3823	6022	4.31	0.03	1.39
HD4307	5812	4.1	0.05	1.22
HD4915	5658	4.52	0.06	0.9
HD55	4679	4.51	0.07	0.05
HD6348	5107	4.51	0.09	0.07
HD6673	4960	4.49	0.09	0.58
HD6735	6082	4.49	0.1	1.15
HD7134	5940	4.41	0.12	1.17
HD7199	5386	4.34	0.12	1.01
HD7449	6024	4.51	0.12	1.11

HD750	5060	4.39	0.13	0.59
HD8326	4971	4.48	0.15	0.81
HD8389A	5283	4.37	0.15	1.06
HD8406	5726	4.5	0.15	0.87
HD8638	5507	4.43	0.16	0.74
HD870	5381	4.42	0.16	0.79
HD8828	5403	4.46	0.17	0.72
HD8859	5502	4.41	0.17	0.77
HD8912	5211	4.43	0.18	0.7
HD9246	4999	4.49	0.2	0.13
HD96700	5845	4.39	0.24	1.04
HD9782	6023	4.42	0.25	1.09
HD9796	5179	4.38	0.25	0.66
HD191902	4691	4.25	-0.15	0.31
HD192117	5479	4.48	-0.14	0.75
HD192310	5166	4.51	-0.14	0.97
HD195564	5676	4.03	-0.13	1.11
HD198075	5846	4.56	-0.12	0.95

Appendix 2. Table of our result derived by two Ca I lines at λ6439.08 Å and λ6122.21 Å.

Star	Logg (6439.08)	Logg (6122.21)	Av.logg	sigma	logg (Sousa)
HD21938	3.9683	3.72584	3.84707	0.12123	4.38
HD21019	3.34854	3.29253	3.320535	0.028005	3.93
HD27471	4.20873	4.17637	4.19255	0.01618	4.25
HD19423	4.14979	4.08387	4.11683	0.03296	4.23
HD21161	4.35926	4.38318	4.37122	0.01196	4.24
HD29263	4.39681	4.16678	4.281795	0.115015	4.35
HD31103	4.65324	4.63391	4.643575	0.009665	4.49
HD28969	4.34359	4.91045	4.62702	0.28343	4.68
HD21977	4.54981	4.46218	4.505995	0.043815	4.45
HD19641	4.52544	4.33559	4.430515	0.094925	4.39
HD18083	4.83241	3.39512	4.113765	0.718645	4.7
HD29303	4.35201	4.29583	4.32392	0.02809	4.52
HD24085	4.73824	4.72728	4.73276	0.00548	4.47
HD23901	3.49926	3.49241	3.495835	0.003425	3.93
HD29428	4.51237	4.31652	4.414445	0.097925	4.48
HD29137	4.43861	4.38069	4.40965	0.02896	4.28
HD25912	4.71484	4.62608	4.67046	0.04438	4.52
HD22177	4.46034	4.31977	4.390055	0.070285	4.26
HD27063	4.62713	4.46674	4.546935	0.080195	4.44
HD26729	4.38874	4.39277	4.390755	0.002015	4.17
HD22249	4.68264	4.57768	4.63016	0.05248	4.63
HD28254	4.46461	4.38728	4.425945	0.038665	4.15
HD28185	4.5813	4.45855	4.519925	0.061375	4.42
HD21411	4.36021	4.25383	4.30702	0.05319	4.51
HD24558	4.07921	3.8762	3.977705	0.101505	4.4
HD20003	4.61619	4.34013	4.47816	0.13803	4.41
HD30177	4.66258	4.44947	4.556025	0.106555	4.34
HD30306	4.50669	4.34105	4.42387	0.08282	4.32
HD22282	4.34717	4.31064	4.328905	0.018265	4.32

HD21693	4.53204	4.31927	4.425655	0.106385	4.37
HD23249	4.05804	3.88939	3.973715	0.084325	3.89
HD21759	4.0397	3.93641	3.988055	0.051645	4.49
HD30669	4.59004	4.39318	4.49161	0.09843	4.37
HD18386	4.75094	4.61996	4.68545	0.06549	4.39
HD19230	4.5622	4.25283	4.407515	0.154685	4.63
HD25105	4.5142	4.29006	4.40213	0.11207	4.47
HD25673	4.19376	4.01441	4.104085	0.089675	4.47
HD20781	4.51722	4.3299	4.42356	0.09366	4.37
HD18822	4.6464	4.42044	4.53342	0.11298	4.43
HD24633	4.64927	4.3894	4.519335	0.129935	4.36
HD26965A	4.35929	4.24911	4.3042	0.05509	4.39
HD30858	4.48927	4.29691	4.39309	0.09618	4.45
HD25061	4.66007	4.42994	4.545005	0.115065	4.42
HD18719	4.67638	4.55101	4.613695	0.062685	4.41
HD25565	4.62508	4.47527	4.550175	0.074905	4.47
HD25120	4.52525	4.35763	4.44144	0.08381	4.47
HD22049	4.6776	4.5167	4.59715	0.08045	4.53
HD22610	4.53161	4.29216	4.411885	0.119725	4.44
HD24331	4.37761	4.21503	4.29632	0.08129	4.51
HD18777	4.68855	4.53252	4.610535	0.078015	4.39
HD25357	4.74798	4.64273	4.695355	0.052625	4.72
HD23356	4.55734	4.41373	4.485535	0.071805	4.5
HD21251	4.56835	4.29658	4.432465	0.135885	4.41
HD23472	4.51942	4.28325	4.401335	0.118085	4.38
HD22897	4.54715	4.37105	4.4591	0.08805	4.44
HD20868	4.63841	4.38739	4.5129	0.12551	4.26
HD20492	4.68898	4.40065	4.544815	0.144165	4.3
HD21209A	4.43775	4.18335	4.31055	0.1272	4.31
HD21749	4.48208	4.43576	4.45892	0.02316	4.4
HD30523	4.70114	4.29653	4.498835	0.202305	4.57
HD967	3.75288	3.49032	3.6216	0.13128	4.53
HD1320	4.34147	4.23945	4.29046	0.05101	4.49
HD1461	4.5246	4.55449	4.539545	0.014945	4.38

HD8859	3.99816	4.0068	4.00248	0.00432	4.41
HD283	3.88459	3.84229	3.86344	0.02115	4.51
HD6348	3.8588	3.7213	3.79005	0.06875	4.51
HD870	4.25933	4.17467	4.217	0.04233	4.42
HD9796	3.99803	3.87184	3.934935	0.063095	4.38
HD3569	4.1162	4.04715	4.081675	0.034525	4.54
HD10166	4.71285	4.4278	4.570325	0.142525	4.48
HD9246	3.75763	3.77696	3.767295	0.009665	4.49
HD7199	4.53193	4.39352	4.462725	0.069205	4.34
HD8912	4.22529	4.11255	4.16892	0.05637	4.43
HD750	4.05297	3.9212	3.987085	0.065885	4.39
HD13060	4.71386	4.6426	4.67823	0.03563	4.34
HD13808	4.43661	4.33207	4.38434	0.05227	4.4
HD8389A	4.53529	4.3452	4.440245	0.095045	4.37
HD11683	4.58714	4.41456	4.50085	0.08629	4.42
HD6673	4.21125	4.00655	4.1089	0.10235	4.49
HD2025	4.35977	4.19885	4.27931	0.08046	4.58
HD55	3.82793	3.77643	3.80218	0.02575	4.51
HD8326	4.46859	4.16591	4.31725	0.15134	4.48
HD12617	4.88505	4.62683	4.75594	0.12911	4.46
HD13789	4.55652	4.08315	4.319835	0.236685	4.33
HD191902	4.36527	4.13997	4.25262	0.11265	4.25
HD192117	4.65918	4.40064	4.52991	0.12927	4.48
HD192310	4.76812	4.5756	4.67186	0.09626	4.51
HD195564	4.23735	4.08209	4.15972	0.07763	4.03
HD198075	4.43672	4.23499	4.335855	0.100865	4.56